JBC Papers in Press. Published on December 4, 2015 as Manuscript M115.684597
The latest version is at http://www.jbc.org/cgi/doi/10.1074/jbc.M115.684597

Mycobacterium tuberculosis WhiB3 responds to vacuolar pH- induced changes in mycothiol redox potential to modulate phagosomal maturation and virulence

Mansi Mehta[1, 2], Raju. S. Rajmani[1], and Amit Singh[1*]

Affiliation: [1]Department of Microbiology and Cell Biology (MCBL), Centre for Infectious Disease Research (CIDR), Indian Institute of Science, Bangalore-12, India, [2]International Centre for Genetic Engineering and Biotechnology (ICGEB), New Delhi-67.

***Correspondence:** Amit Singh (Assistant Professor), Department of Microbiology and Cell Biology, IISc, Bangalore-12, email: asingh@mcbl.iisc.ernet.in, Tel: 91-80-22932604.

Keywords: *Mycobacterium tuberculosis*, redox signaling, pH regulation, virulence factor, lysosomal acidification

ABSTRACT

The ability of *Mycobacterium tuberculosis* (*Mtb*) to resist intraphagosomal stresses such as oxygen radicals and low pH is critical for its persistence. Here, we show that a cytoplasmic redox sensor, WhiB3, and the major *Mtb* thiol, mycothiol (MSH), are required to resist acidic stress during infection. WhiB3 regulates the expression of genes involved in lipid anabolism, secretion, and redox metabolism, in response to acidic pH. Furthermore, inactivation of MSH pathway subverted the expression of *whiB3* along with other pH-specific genes in *Mtb*. Using a genetic biosensor of mycothiol redox potential (E_{MSH}), we demonstrated that a modest decrease in phagosomal pH is sufficient to generate redox heterogeneity in E_{MSH} of the *Mtb* population in a WhiB3-dependent manner. Data indicate that *Mtb* needs low pH as a signal to alter cytoplasmic E_{MSH}, which activates WhiB3-mediated gene expression and acid resistance. Importantly, WhiB3 regulates intraphagosomal pH by down-regulating the expression of innate immune genes and blocking phagosomal maturation. We show that this block in phagosomal maturation is in part due to WhiB3-dependant production of polyketide lipids. Consistent with these observations, *MtbΔwhiB3* displayed intramacrophage survival defect, which can be rescued by pharmacological inhibition of phagosomal acidification. Lastly, *MtbΔwhiB3* exhibited marked attenuation in the lungs of guinea pigs. Altogether, our study revealed an intimate link between vacuolar acidification, redox physiology, and virulence in *Mtb*, and discovered WhiB3 as crucial mediator of phagosomal maturation arrest and acid resistance in *Mtb*.

INTRODUCTION

Mycobacterium tuberculosis (*Mtb*) causes a chronic persistent infection that affects one third of the world population (www.who.int/tb). Macrophage is the major human host cell for growth, survival, and persistence of *Mtb*. Studies indicate that *Mtb* continuously senses the phagosomal environment and modulates genetic pathways to regulate intramacrophage growth for long term persistence (1-3). In this regard, acidic pH has recently been appreciated as an important intraphagosomal signal sensed by *Mtb* to regulate gene expression and establish chronic infection (3). The importance of pH emerged from several studies showing that pathogenic mycobacteria successfully restrict fusion of phagosomes with acidic lysosomes and therefore multiply in a growth permissive vacuolar compartment with a pH of ~6.2 (4-6). However, upon activation of macrophages by interferon-gamma (IFN-γ), and *Escherichia coli*-derived lipopolysaccharide (LPS), the pH of *Mtb*'s phagosome drops to <5.0,

resulting in *Mtb* growth restriction (6-8). Hence, the inhibition of phagosomal maturation during early stages of infection and induction of acid resistance mechanisms later during immune-activation are considered major virulence strategies adopted by *Mtb* to establish chronic infection (9). Despite the recognized role of acidic pH in regulating *Mtb* pathogenesis, the mechanisms by which *Mtb* responds to fluctuations in phagosomal pH and calibrates its gene expression for intracellular growth and persistence remain poorly characterized.

Recent studies indicate that *Mtb* maintains a neutral intrabacterial pH (~7.2) after exposure to a range of acidic pHs (6.2 to 4.5) *in vitro*, and inside the acidic phagosomal milieu of resting or activated macrophage (10). This indicates that *Mtb* stably maintains intrabacterial pH homeostasis during infection and, therefore, the intrabacterial pH *per se* is unlikely to be the signal that triggers alterations in *Mtb*'s gene expression in response to changes in phagosomal acidity. Therefore novel insights are needed to discover which aspects of mycobacterial physiology are modulated by phagosomal acidity and what are the bacterial sensors of phagosomal pH. In this context, a Fe-S cluster containing putative transcription factor, WhiB3, is induced in response to acidic pH in medium, inside macrophages, and in the lungs of infected animals (11,12). In fact, *whiB3* was the only transcription factor whose expression was found to be pH-responsive inside macrophages. *In vitro* studies have shown that WhiB3 responds to dormancy signals such as O_2 and nitric oxide (NO) via its 4Fe-4S cluster (13). However, phenotypic experiments revealed no role of WhiB3 in controlling mycobacterial survival in response to NO or hypoxia (13). Therefore, how WhiB3 regulates mycobacterial persistence remained uncharacterized. Consistent induction of *whiB3* in acidic environments *in vitro* and inside macrophages (12) implicated WhiB3 in regulating adaptation of *Mtb* in response to phagosomal pH. A fundamentally important question remains yet unanswered: What is the mechanism by which WhiB3 mediates the acid response of *Mtb* during infection?

In this study, we performed global microarray analysis to identify genes regulated by WhiB3 in response to acid stress. More-importantly, we measured the dynamic changes in mycothiol redox potential (E_{MSH}) of wt *Mtb* and *MtbΔwhiB3*in response to acidic pH *in vitro*, and inside naïve and activated macrophages. Confocal studies and host microarray studies were performed to examine the function of WhiB3in regulating phagosomal maturation. Lastly, the physiological importance of *whiB3*-mediated effects on gene expression, redox homeostasis, and phagosomal maturation was investigated by performing survival studies in macrophages and guinea pigs. Our study, for the first time, demonstrates how *Mtb* recalibrates its redox physiology in response to vacuolar pH during infection and identifies a major role of WhiB3 in responding to acidic stress.

EXPERIMENTAL PROCEDURES

Bacterial strains and growth conditions

Wild type *M.tuberculosis* H37Rv (*wt Mtb*), *MtbΔwhiB3*, and *whiB3-comp* strains were cultivated as described (13). *E. coli* cultures were grown in LB medium. When required, culture medium was supplemented with kanamycin (25 µg/ml) or hygromycin (50 µg/ml). For acid stress, the pH of 7H9 broth was adjusted using hydrochloric acid (HCl) and buffered using 100 mM 2-(4-morpholino)-ethane sulfonic acid (MES). Approximately $1x10^7$ cells/ml were exposed to various pH adjusted media and survival was monitored at day 0 and day 4 by serially diluting the culture and enumerating colony forming units (CFUs). For CCCP (Carbonyl cyanide m-chlorophenylhydrazone) treatment, bacteria were treated with 500µM CCCP for 4 h.

Generation of *MtbΔwhiB3* and *whiB3* Complemented strains

For constructing *MtbΔwhiB3*, 1-kb left (LF) and right (RF) flanking regions of *whiB3* (Rv3416) were cloned upstream and downstream of loxP-*gfp*-hygromycin-loxP cassette in a mycobacterial *sacB* based suicidal vector, pML523

(a kind gift from Michael Neiderwies, UAB, USA). The construct was digested with *Spe*I and *Nsi*I to release LF and RF regions of *whiB3* along with loxP-*gfp*-hygromycin-loxP cassette, blunt-ended and cloned into *Eco*RV/*Pst*I digested pRSF-duet vector (Clontech). The pRSF-*whiB3*clonewas pre-treated with UV as described previously (14)and electroporated into wt *Mtb* for allelic exchange. The resulted *MtbΔwhiB3* ($Hyg^RKan^SGFP^+$) colonies were screened by antibiotic selection and verified by PCR. To unmark *MtbΔwhiB3* strain, pCRE-ZEO-SacB (a gift from Dr. Amit Pandey, THSTI, Haryana, India) was electroporated into *MtbΔwhiB3*and loxP-*gfp*-hygromycin-loxP cassette was released from the genome. The resulting unmarked *MtbΔwhiB3* strain was confirmed by the absence of antibiotic selection marker. Disruption of *whiB3* was confirmed by quantitative real time PCR (qRT-PCR).

For constructing *whiB3-comp* strain, *whiB3* gene along with its promoter region was amplified from *Mtb* genome and inserted into an *E.coli*-Mycobacterial shuttle vector, pSD5. The pSD-*whiB3* clone was electroporated into unmarked *MtbΔwhiB3* strain to generate *whiB3-comp* strain. Expression of *whiB3* in the *whiB3-comp* strain was confirmed by qRT-PCR.

Cell Lines

The human monocytic cell line THP-1 and mice RAW 264.7 macrophages were cultivated as described previously (15).RAW 264.7 macrophages were activated using 100 ng/ml IFN-γ and 20 ng/ml LPS.

Antibodies and reagents

Antibodies for mammalian markers [CD63, vacuolar H^+-ATPase (V-ATPase)] were purchased from Santa Cruz Biotechnology. Lysotracker® DND –red99 was purchased from Molecular Probes, Invitrogen. Secondary Antibody Alexa Fluor 568 was purchased from Molecular Probes, Invitrogen. Fluorescein 5(6)-isothiocyanate was purchased from Sigma Aldrich. Bafilomycin A1 was purchased from Invivogen, and stocks were made in dimethyl sulfoxide (DMSO), aliquoted and stored at -20°C.

Growth conditions for qRT-PCR and Microarray analysis

For analyzing the influence of acid stress on gene expression, *Mtb* strains (*Mtb*, *MtbΔwhiB3*, *MtbΔmshA*) were grown till an O.D. $_{600nm}$ of 0.3-0.4 and exposed to 7H9 medium adjusted to a range of acidic pH 4.5, 5.5, 6.2, 7.0 and normal 7H9 (6.6) for 2 h at 150 rpm at 37°C. Total RNA from wt *Mtb* and *MtbΔwhiB3* (pH 4.5 and pH 6.6) was processed and hybridized to *Mtb* Whole Genome Gene Expression Profiling microarray-G2509F (AMADID: G2509F_034585, Agilent Technologies PLC). DNA microarrays were provided by University of Delhi South Campus MicroArray Centre (UDSCMAC). RNA amplification, cDNA labeling, microarray hybridization, scanning and data analysis were performed at the UDSCMAC as described (16). Slides were scanned on a microarray scanner (Agilent Technologies) and analyzed using the GeneSpring software. Results were analysed in MeV with Significance Analysis of Microarrays considered significant at $p \leq 0.05$. The normalized data from the microarray gene expression experiment has been submitted to NCBI's Gene Expression Omnibus (GEO, http://www.ncbi.nlm.nih.gov/geo/) and can be queried via GEO series accession number GSE61579.

qRT-PCR

First-strand cDNA synthesis was performed using 500 ng of the total RNA with iScript Select cDNA Synthesis Kit (Bio-Rad) using random oligonucleotide primers. PCR was performed using gene specific primers (Table 1). Gene expression was analyzed with real-time PCR using iQTM SYBR Green Supermix (Bio-Rad) and a CFX96 RT-PCR system (Bio-Rad). Data analysis was performed with the CFX Manager™ software (Bio-Rad). For comparison between *wt Mtb*, *MtbΔwhiB3*, and the *whiB3-comp* strains, the induction ratio for each gene was normalized to wt *Mtb* 16S rRNA expression.

Measurement of intramycobacterial E_{MSH} *in vitro* and during infection

For intramycobacterial E_{MSH} determination, various strains expressing Mrx1-roGFP2 were cultured and exposed to pH stress as indicated in the previous section. At indicated time points, cells were treated with 10 mM N-Ethylmaleimide (NEM) for 5 min at room temperature (RT) and fixed with 4% paraformaldehyde (PFA) for 15 min at RT. After washing thrice with 1X phosphate buffer saline (PBS), bacilli were analyzed using FACS Verse Flow cytometer (BD Biosciences). The biosensor response was measured by analyzing the ratio at a fixed emission (510 nm) after excitation at 405 and 488 nm. Data was analyzed using the FACSuite software. Intramycobacterial E_{MSH} was measured using Nernst Equation as described earlier (15).

For measuring intramycobacterial E_{MSH} during infection, PMA-differentiated THP-1 cells were infected with wt *Mtb*, *MtbΔwhiB3* and *whiB3-comp* strains expressing Mrx1-roGFP2 at a multiplicity of infection (moi: 10).Infected macrophages were treated with NEM-PFA, washed with 1X PBS, and analyzed by flow cytometry as described previously(15). In case of Bafilomycin A1 (BafA1) treatment, THP-1 cells were treated with 10 nM BafA1 (Invivogen) or DMSO (vehicle control) 1 h prior to infection and processed for infection and sample preparation as described above.

Survival of *Mtb* strains in macrophages

PMA-differentiated THP-1 monocytes and IFNγ+LPS activated RAW 264.7 macrophages were infected with wt *Mtb*, *MtbΔwhiB3* and *whiB3-comp* strains at a moi of 2 for 4 h, followed by treatment with 200 µg/ml amikacin to remove extracellular bacteria. For BafA1 experiments, THP-1 cells were treated with 10 nM BafA1 or DMSO (vehicle control) 1 h prior to infection. Cells were maintained in BafA1 throughout the experiment. After infection, cells were washed thoroughly with warm RPMI medium and resuspended in 10% RPMI medium containing BafA1 or DMSO as per requirements. Samples were collected at indicated time points, lysed using 0.06 % SDS-7H9, serially diluted in 7H9, plated on OADC-7H11 agar medium and incubated at 37°C incubator. Colonies were counted after 3 weeks post plating.

Isolation of wt *Mtb* surface exposed polyketide lipids

50 ml wt *Mtb* was grown in 37˚C shaker incubator till mid-log phase ($O.D._{600\ nm}$ 0.5-0.8). Surface exposed extractable total lipids were isolated as described previously (17). For lipid complementation assays, 100 µg/ml lipids were coated on the coverslips, THP-1 were seeded, PMA-differentiated and infected with *MtbΔwhiB3*as done above.

Confocal Microscopy

Logarithmically grown *Mtb* strains were stained with Fluorescein isothiocyanate (FITC) as described earlier (18). PMA-differentiated THP-1 cells ($0.25x10^6$) were seeded, and infection was done with wt *Mtb*, *MtbΔwhiB3, whiB3-comp* strains at a moi of 10 as described elsewhere(19). 1 h prior to the time point, the media of the cells was replaced with complete media containing 100 nM Lysotracker® Red DND-99. Staining for CD63 and H+ V-ATPase was started with fixative treatment (4% PFA in 1X PBS) for 15 min, followed by permeabilization (0.2% triton -100 in 1X PBS), and blocking (3% BSA and 0.5% tween-80 in 1X PBS). Samples were stained with primary antibodies (anti-CD63 and anti-V-ATPase) followed by secondary antibodies, and followed by mounting using ProLong® Antifade Reagent (Molecular Probes, Invitrogen). The stained cells were visualized under Leica TCS SP5 Confocal Microscope. Z stacks were taken, collapsed to 2D image and analyzed by LAS AF Version: 2.6.0 build 7266. All the z stacks were taken at 63X oil immersion objective (with zoom). A minimum of five fields were captured and at least 50 macrophages were analyzed for all the phagosomal markers, accounting an approximate analysis of ~100-200 bacteria per well. For each experimental group, a minimum of three replicates was scored.

THP-1 microarrays

The infection of THP-1 monocytic cells followed by RNA isolation, sample processing, and hybridization (Illumina Human-Ht-12 BeadChip) were performed as described earlier (19). Array data processing was performed on Illumina Bead Studio software. Expression analysis was done using Volcano plot based approach using fold change > 1.5 and p value > 0.05 as cut-off. Differentially Expressed gene taken for Significant Biological analysis was done using tool GO-Elite (1.2.5 V) with z score > 1.96 and p value < 0.05 as cutoffs. The normalized data from the microarray gene expression experiment can be queried via GEO series accession number GSE65714.

Aerosol infection of guinea pigs

Outbred Hartley guinea pigs (~300–400 g body weight) were given a low dose of logarithmic phase grown cultures of wt *Mtb, MtbΔwhiB3* and *whiB3-comp*, using a Madison chamber aerosol generation instrument calibrated to deliver 50–100 CFU per animal lung. Animals were sacrificed (n=5) at 1, 30 and 60 days p.i. for determination of organ bacterial burden and histopathology analysis. Histopathology analysis was performed as described previously (14). A blinded examination of at least three serial sections from each guinea pig was carried out.

Statistical analysis

Statistical analyses were conducted using Graphpad Prism software and values were presented as mean ± SD. The statistical significance of the differences between experimental groups was determined by two-tailed, unpaired student's *t*-test. Differences with a p value of <0.05 were considered significant.

RESULTS

***Mtb* WhiB3 regulates survival and gene expression in response to acidic pH**

Recent studies indicated that intraphagosomal pH might be one of the earliest cues to which *Mtb* responds and realigns its transcriptional programming (12). Microarray studies have revealed that the expression of *whiB3* was induced early in macrophages in a pH-dependent manner (12). We also found an ~2-, 4-, and 35-fold increased expression of *whiB3* as compared to 16srRNA at pHs 6.2, 5.5, and 4.5, respectively.

Given the sustained induction of *whiB3* in response to acidic pH, we reasoned that WhiB3 might play an important role in tolerating acid stress. We generated an unmarked strain of *Mtb* lacking the entire open reading frame (ORF) of *whiB3*and putative *MtbΔwhiB3* clones were verified by PCR (Fig. 1A, 1B and 1C). We monitored the survival of wt *Mtb*, *MtbΔwhiB3, whiB3-comp* in 7H9-Tyloxapol (7H9-Ty) medium adjusted to pH of 6.6 (normal 7H9), 5.5, and 4.5. At day 4 post-treatment, survival at various pH stress conditions was monitored by enumerating CFUs. We observed that *MtbΔwhiB3* survived to a level comparable to wt *Mtb* at pH 6.6 and 5.5 (Fig. 1D). However, it displayed an ~55 -fold reduction in its survival at pH 4.5 as compared to wt *Mtb* (p value= 0.007; Fig.1D). Stable expression of *whiB3* in *MtbΔwhiB3* resulted in a significant complementation of this survival defect (Fig. 1D). These observations confirmed that not only *whiB3* expression is induced by acidic pH, it is also required for growth in acidic environments *in vitro*.

Next, we sought to determine the role of WhiB3 in controlling pH-specific gene expression. We minimized any contributions of pH-induced cell death on gene expression by performing microarrays at an early time point (2 h) post exposure to pH 4.5. Expression data revealed differential regulation of several genes involved in secretion, central metabolism/oxidative phosphorylation, lipid metabolism, amino acid metabolism, cell wall biosynthesis/membrane transporters, and gene regulation at pH 4.5 as compared to pH 6.6 (Fig. 2A, 2B and Table S1).

Surprisingly, genes directly implicated in mitigating redox stress in *Mtb* were also influenced

by acid stress. For example, expression of major antioxidant genes including thioredoxins (*trxB1, trxB2, trxC*), superoxide dismutase (*sodA*), MSH synthesis (*mshB, mca*), and rubredoxin (*rubA, rubB*) was elevated by acidic condition (Table S1). Genes associated with biosynthesis of redox-active amino acids (cysteine and methionine), DNA repair (*recR, dnaK, dnaJ, ogt,*), and NAD^+/NADH balance (*ndh*) were also upregulated (Fig. 2B and Table S1). Noticeably, the expression of *whiB3* was induced to a highest degree among other transcriptional regulators (Table S1). To understand the physiological basis of our findings, we performed a comparative gene expression analysis at pH 4.5 *in vitro* with the transcriptional changes in wt *Mtb* in response to early phagosomal acidity (12). We observed that out of 22 genes that were induced by early phagosomal acidity (12), 17 were also induced by pH 4.5 (≥2- fold, $p<0.05$) (Fig. 2C).

Subsequently, we examined the role of WhiB3 in regulating pH-induced changes in gene expression. In *MtbΔwhiB3,* the expression of 70 pH-induced and 27 pH-repressed genes showed 2-fold ($p<0.05$) differential expression as compared to wt *Mtb* (Table S1). Several genes exhibited pH-specific induction only in wt *Mtb*, whereas they were constitutively expressed in *MtbΔwhiB3*. This includes genes involved in the biosynthesis of complex polyketide lipids; SL-1 (*pks2*), PAT/DAT (*pks3-pks4*), and cysteine metabolism (*cysW, cysN, cysA1, metZ*), (Fig. 2B and Table S1). Genes involved in amino acid biosynthesis (*metH, metK, sahH*), ESX-1 secretion (Rv3614c-Rv3616c), MSH antioxidant system (*mca*, *mtr*), nitrite transport (*narK1*), and leucine biosynthesis (*leuB*) were up-regulated significantly more in wt *Mtb* as compared to *MtbΔwhiB3* at pH 4.5 (Fig. 2B and Table S1). A large subset of genes was upregulated to a higher degree in *MtbΔwhiB3* as compared to wt *Mtb* at acidic pH, indicating the role of WhiB3 in fine tuning the expression of pH-inducible genes. This includes PE-PPE family (*PE-24, PE-8, PE-32, PPE-65, PPE-31*), protein biosynthesis (*rpmH, rplU, rplY*), and transcriptional regulators (*whiB7,* Rv0827c*,* Rv3183) (Table S1). Since induction of *whiB3* was responsive to early phagosomal acidity (12), we checked the expression status of other phagosomal-responsive genes in *MtbΔwhiB3*. We discovered that out of 22 phagosomal pH responsive genes, expression of 16 was controlled by WhiB3 (Fig. 2C, ≥1.5-fold, p value ≤0.05). Lastly, microarray data was validated by measuring the expression of a selected set of pH- and *whiB3*-dependent genes by qRT-PCR (Table 2).Taken together, our results implicate WhiB3 in controlling survival and expression of genes involved in altering cell wall lipids composition, secretion, and redox balance in response to acid stress.

Acidic pH induces dynamic changes in mycothiol redox potential (E_{MSH}) of *Mtb* in a WhiB3-dependent manner

Since WhiB3 is believed to serve as an intracellular redox sensor in *Mtb*, we hypothesized that it might regulate gene expression by responding to pH-induced changes in intramycobacterial redox physiology. Therefore, we precisely measured the dynamic changes in mycothiol redox potential (E_{MSH}) of wt *Mtb*, *MtbΔwhiB3*, and *whiB3-comp* strains in response to a range of pH conditions *in vitro*. We exploited a highly sensitive, specific, and non-invasive biosensor of E_{MSH} (Mrx1-roGFP2) in mycobacteria (15). Mycothiol (MSH) is the most abundant low molecular weight thiol produced by mycobacteria (15). Therefore, E_{MSH} measurement provides a reliable and sensitive numerical evaluation of cytoplasmic redox state of mycobacteria. The biosensor shows increase in fluorescence excitation ratio at 405/488 nm upon oxidative stress, whereas a ratiometric decrease is associated with reductive stress (15).

Wt *Mtb*, *MtbΔwhiB3*, and *whiB3-comp* expressing Mrx1-roGFP2 were exposed to a gradient of pH conditions (pH of 7.0, 6.2, 5.5, and 4.5) and the ratiometric response was measured by flow cytometry at various time points. By fitting ratiometric intensities into Nernst equation, we precisely measured the E_{MSH} of *Mtb* strains at various pH conditions (see *Experimental procedures*). We found that the steady-state E_{MSH}

of wt *Mtb*, *MtbΔwhiB3*, and *whiB3-comp* strains at the neutral pH to be ~ -275 mV (Fig. 3A). The comparable E_{MSH} of *MtbΔwhiB3* and wt *Mtb* indicates that WhiB3 is not required for maintaining ambient E_{MSH} of *Mtb* at neutral pH. Interestingly, 24 h exposure of wt *Mtb* to either pH 6.2or 5.5 or 4.5 resulted in a significant decrease in intramycobacterial E_{MSH} (~ -305±0.7 mV), indicating that transition from neutral to either milder or harsher acidic pH conditions uniformly induces reductive-E_{MSH} in *Mtb* (Fig. 3B, 3C and 3D). Moreover, pH-exposed wt *Mtb* largely maintained E_{MSH}-reduced throughout the course of experiment. We noted a very modest recovery from reductive-E_{MSH} (*i.e.* ~ -295 mV) at pH 6.2 and 5.5 at later time points, whereas no such effect was observed at pH 4.5 (Fig. 3B, 3C, and 3D). Importantly, while changes in intramycobacterial E_{MSH} for *MtbΔwhiB3* mostly followed wt *Mtb* pattern at pH 6.2 (Fig. 3B), distinct redox deviations were observed at pH 5.5 and 4.5. For example, at pH 5.5, *MtbΔwhiB3* displayed a relatively lesser decrease in intramycobacterial E_{MSH} (-297 mV±0.7) at 24 h followed by a slightly better recovery at 48-72 h (~ -287 mV±0.7) as compared to wt *Mtb* (Fig. 3C). Noticeably, exposure of *MtbΔwhiB3* to pH 4.5 displayed only a marginal decrease in E_{MSH} (-287 mV±1.5) at 24 h followed by a significant increase in intramycobacterial E_{MSH} (-260.5 mV±3.5) at 48 and (-266 mV±0.7) 72 h as compared to wt *Mtb*, suggesting an overall oxidative shift in E_{MSH} of *MtbΔwhiB3* (Fig. 3D). The complemented strain showed changes in intramycobacterial E_{MSH} that were comparable to wt *Mtb* (Fig. 3A, 3B, 3C, and 3D). These results indicate that acidic pH perturbs redox physiology of *Mtb* by inducing reductive shift in intramycobacterial E_{MSH} and that the loss of WhiB3 impaired the ability of *Mtb* to orchestrate an efficient and dynamic MSH-specific reductive response upon acid stress.

Above results point towards a pH-mediated reductive shift in E_{MSH} of *Mtb* that might acts as a signal for WhiB3 to regulate gene expression. We reasoned that disruption of MSH reductive pathway would provide an ideal opportunity to study, in parallel, the effect of reductive E_{MSH} on pH-specific gene expression. Therefore, we expressed Mrx1-roGFP2 in MSH-deficient *Mtb* strain (*MtbΔmshA*) and found that E_{MSH} of the strain remained oxidized (~ >-240 mV) at various pH conditions (7.0, 6.2, 5.5, and 4.5). Next, we analyzed the expression of a set of pH-inducible genes in a MSH-deficient *Mtb* strain (*MtbΔmshA*) by qRT-PCR. At pH 7.0, expression of pH-inducible genes in *MtbΔmshA* is comparable to wt *Mtb* (Table 2). In contrast, expression of pH-inducible genes did not show any up-regulation in *MtbΔmshA* at pH 4.5 (Table 2). More importantly, the expression of *whiB3* was ~37-fold down-regulated in *MtbΔmshA* at pH 4.5 (Table 2). These results, along with our microarray data showing *whiB3*-dependent expression of MSH biosynthetic genes, suggest that MSH and WhiB3 are the components of a regulatory circuit mediating gene expression upon acid stress.

Dissipation of pH-gradient perturbs pH-specific induction of reductive-E_{MSH} in *Mtb*

Excess increase in intracellular acidity can damage DNA, proteins, and lipids to exert bacterial killing. However, whether acid is the main effectors of bacterial killing in response to pH stress is not clear. Because *Mtb* maintains cytoplasmic pH homeostasis even under severe pH stress, how increase in internal acidity affects mycobacterial redox physiology and survival is not studied. To examine the influence of elevated cytoplasmic acidity on intramycobacterial redox potential, we cultured *Mtb* strains at various pH for 72 h as described in the previous section, and disrupted pH homeostasis by discharging the pH gradient (ΔpH) using a well known protonophore, CCCP. Treatment with 500 µM of CCCP for 4 h is sufficient to permeate the cell wall of mycobacteria and equilibrates cytoplasmic pH with the external pH (20). We followed intramycobacterial E_{MSH} and viability of *Mtb* strains at 4 h post-treatment with 500 µM CCCP. Expectedly, at pH 7.0, treatment with CCCP has no effect on either intramycobacterial E_{MSH} or viability of *Mtb* (Fig. 3A and 3E). At pH 6.2, CCCP treatment triggers a moderate recovery from reductive shift in E_{MSH} of wt *Mtb* (-284mV), *MtbΔwhiB3* (-288 mV), and

whiB3-comp (-280 mV) strains (Fig. 3B). However, under these experimental conditions viability of *Mtb* strains was not significantly compromised (data not shown).Consistent with this pattern, CCCP treatment of *Mtb* strains at pH 5.5 and 4.5 completely reversed the pH-specific increase in reductive-E_{MSH}, as indicated by an increased shift in intramycobacterial E_{MSH} towards oxidizing (ranging from -260 mV to -250 mV) (Fig. 3C and 3D).While an increase in oxidative stress upon CCCP treatment does not significantly influence the viability of *Mtb* strains at pH 5.5 (data not shown), an ~3-4 fold reduction in CFUs was observed at pH 4.5 (Fig. 3F and 3G). Importantly, since CCCP-mediated skew towards E_{MSH}-oxidized was activated at moderate pH values of 5.5, at which ionophore showed no mycobactericidal effect, our results indicate that dissipation of ΔpH and consequent oxidative shift in intramycobacterial E_{MSH} precedes bacterial death. Together, these results suggest that the maintenance of pH homeostasis and the induction of reductive E_{MSH} are effective and overlapping mycobacterial strategies to avoid oxidative stress-mediated death caused by increased internal acidity.

WhiB3 regulates intramycobacterial E_{MSH} and survival during infection

We, next, determined whether WhiB3 regulates intramycobacterial E_{MSH} and survival in the natural context of infection. To investigate this issue, we infected THP-1 macrophages with *Mtb* strains expressing Mrx1-roGFP2 at a moi of 10 and monitored intramycobacterial E_{MSH} and survival, as described previously (15).

As expected, *Mtb* strains displayed subpopulations with oxidized (−240±3 mV), reduced (−300±6 mV), and basal (−275±5 mV) E_{MSH} inside THP-1 cells (15). The wt *Mtb* displayed a gradual increase in population with E_{MSH}-reduced(~30-65%) at initial time points (0-24 h p.i), followed by an increase in E_{MSH}-oxidized (~20%) at the intermediate period (48h p.i) and recovery from oxidative stress at 72 h p.i. (Fig.4A). In contrast to what was observed with *whiB3*-sufficient strains (wt *Mtb*, *whiB3-comp)*, *MtbΔwhiB3* showed negligible proportions of E_{MSH}-reduced bacteria and a greater fraction of bacteria with E_{MSH}-oxidized, at each time point examined (Fig. 4A, 4B, and 4C). The defective ability of *MtbΔwhiB3* to maintain reductive-E_{MSH} correlated with a significant growth defect in its survival inside THP-1 macrophages as compared to wt *Mtb* and*whiB3-comp* (Fig. 4D).

Activated murine macrophages are known to control mycobacterial survival by generating excessive acid, ROS, and RNS stress (1).To investigate the role of WhiB3 in controlling E_{MSH} of *Mtb* upon stimulation of antimycobacterial stresses, we infected IFN-γ and LPS activated RAW264.7 cells with wt *Mtb*, *MtbΔwhiB3*, and *whiB3-comp* at a moi of 10 and measured the intramycobacterial E_{MSH}. In a parallel experiment, intramacrophage survival of *Mtb* strains was also compared upon immune-activation. We observed a substantial shift in subpopulation with E_{MSH}-oxidized in all three strains (Fig. 4E, 4F, and 4G). However, *MtbΔwhiB3* displayed highest proportion of cells with E_{MSH}-oxidized (Fig. 4F). Inside immune-activated macrophages, wt *Mtb* showed a decline in survival at 48 h p.i. followed by a significant recovery at 96 h p.i. (Fig. 4H). However, while initial killing of *MtbΔwhiB3* was comparable to wt *Mtb*, the mutant showed a 2-fold difference in survival at 96 h p.i. (p= 0.0018) (Fig. 4H). The *whiB3-comp* strain grew equivalent to wt *Mtb* levels inside activated macrophages (Fig. 4H).

An oxidative shift in the E_{MSH} of wt *Mtb* inside activated macrophages, where phagolysosomal pH drops to 4.5, is in contrast with the reductive shift in intramycobacterial E_{MSH} at pH 4.5 in 7H9 culture medium. However, these counter-intuitive findings can be reconciled by the synergistic effect of vacuolar acidification with host ROS and RNS production. In particular, low pH of phagolysosomes allows dismutation of nitrous acid (generated via auto-oxidation of NO) to generate highly toxic nitrogen dioxide (21). Hence, the increase in E_{MSH}–oxidized subpopulations is most likely due to composite response of *Mtb* towards multiple stresses encountered inside activated macrophages.

Altogether, using *in vitro* and macrophage based assays, we demonstrated the role of WhiB3 in mounting efficient antioxidant response to promote intramacrophage survival.

Effect of phagosomal acidification on intramycobacterial E_{MSH} and survival

Since phagosomal pH synergizes with multiple intramacrophage cues such as ROS, and RNS, the specific effect of acidic pH on mycobacterial physiology, gene expression, and survival remain challenging. This has been extremely difficult inside activated macrophages where several mycobactericidal mechanisms (*e.g.* lysosomal hydrolases, ROS, and RNS) are likely to be pH-dependent (21). Therefore, to begin delineating the role of vacuolar acidification on intramycobacterial E_{MSH}, we decided to examine the effect of limited acidification encountered inside THP-1 cells (22). To block phagosomal acidification, we treated THP-1 macrophages with a specific inhibitor of H^+ V-ATPase, BafA1and then infected with *Mtb* strains expressing Mrx1-roGFP2 at a moi of 10. Treatment with 10 nM of BafA1 is known to effectively block phagosomal acidification without affecting macrophage viability during infection with *Mtb* (23). We also observed no influence of 10 nM BafA1 on THP-1 viability (data not shown). Given that *Mtb* phagosomes acidify to pH 6.2-6.4 within minutes of infection (24), we measured intramycobacterial E_{MSH} at initial time points (0 and 24 h p.i.).

In case of wt *Mtb*, BafA1 treatment significantly diminished the proportion of bacilli with E_{MSH}-reduced as compared to untreated macrophages at 0 and 24 h p.i. (Fig. 5A and 5B). Consequent increase in *Mtb* subpopulations with basal-E_{MSH} (similar to 7H9-pH 7.0 grown bacteria) indicates that cells are experiencing near neutral pH in vacuoles upon BafA1 treatment (Fig. 5A and 5B). Importantly, these results indicate that limited acidification encountered inside macrophages is sufficient to induce reductive shift and heterogeneity in E_{MSH} of *Mtb* during infection. In contrast to wt *Mtb*, *MtbΔwhiB3* showed no significant changes in subpopulations with basal, oxidized, and reduced E_{MSH} at 0 and 24 h p.i. upon BafA1 treatment (Fig. 5A and 5B). The *whiB3-comp* strain showed intramycobacterial E_{MSH} changes comparable to wt *Mtb* upon BafA1 treatment (Fig. 5A and 5B). These results suggest that the lack of WhiB3 impaired the ability of *Mtb* to dynamically modulate cytoplasmic E_{MSH} in response to vacuolar pH.

Next, we examined if the inability of *MtbΔwhiB3* to maintain mycothiol redox homeostasis in response to vacuolar acidification was the reason underlying the intramacrophage survival defect of the mutant. To do this, we monitored the survival of wt *Mtb*, *MtbΔwhiB3*, and *whiB3-comp* strains inside untreated and BafA1-treated THP-1 cells by enumerating CFUs at 48 and 96 h p.i. In contrast to defective intramacrophage growth of *MtbΔwhiB3* observed earlier, treatment with BafA1 completely rescued its survival to wt *Mtb* and *whiB3-comp* levels (Fig. 5C). Together, these results indicate the importance of mycothiol redox buffer and WhiB3 in responding to phagosomal acidification and maintaining intramacrophage survival of *Mtb*.

WhiB3 is required to subvert phagosomal acidification

One of the main mechanisms exploited by *Mtb* to resist acid stress is by blocking the normal process of phagosomal maturation to acidified phagolysosomes (4). In this regard, we have shown that the majority of bacilli within acidified phagolysosomal fractions display oxidative-E_{MSH} (15). Because a relatively higher proportion of E_{MSH}-oxidized subpopulations of *MtbΔwhiB3* were detected inside THP-1 cells, we hypothesized that increased fusion of phagosomes containing *MtbΔwhiB3* with acidified lysosomes may be one of the factors that underlies the observed redox variability and intramacrophage survival defect. We, therefore, sought to determine the acidification status of phagosomes containing *MtbΔwhiB3*. To do this, THP-1 macrophages were infected with *Mtb* strains labeled with FITC at a moi of 10 and localization of *Mtb* bacilli was assessed using well-established markers of phagosomal maturation. Localization of *Mtb* bacilli was examined using confocal microscopy. For

measurements, a minimum of five fields per well were captured, and ~ 100-200 bacterium-containing phagosomes were scored per well. For each test group, three replicate wells were scored per experiment.

Staining with Lysotracker revealed that wt *Mtb* largely remained in non-acidified phagosomes with only 25±4% of bacilli colocalized to acidified phagosomes at 24 h p.i (Fig. 6A). In contrast, a significantly greater fraction of *MtbΔwhiB3* (~70%, p value=0.0026) was found in acidified phagosomes and this phenotype was significantly reversed in the complemented strain (Fig. 6A). It has been shown that *Mtb* actively inhibits phagosome acidification by preventing recruitment and/or inducing degradation of a molecular proton motor, H^+ V-ATPase (24, 25). Therefore, we questioned if the increased association of *MtbΔwhiB3* with acidified phagosomes correlates with greater H^+ V-ATPase association. Infected THP-1 macrophages were immuno-stained for human H^+ V-ATPase, and colocalization was measured at 24 h p.i. A significantly greater percentage of phagosomes containing *MtbΔwhiB3* were found to be positive for H^+V-ATPase (~43%±10) as compared to wt *Mtb* (~11%±12) or *whiB3-comp* (~25%±10) (Fig. 6B). Since phagosome acidification is relatively an early step in phagosomal maturation, we next analyzed the status of *MtbΔwhiB3*-containing phagosomes for the late endosome-lysosome fusion markers, CD63. It has been reported that wt *Mtb* prevents phagosomes to mature into CD63 positive state (26). Consistent with our earlier results, ~53%±2 of *MtbΔwhiB3*-containing phagosomes acquired CD63 as compared to ~8%±3 and 31%±4 in the case of wt *Mtb* and *whiB3-comp* strains, respectively (Fig. 6C). The observed differences in the phagosomes of *MtbΔwhiB3* were confirmed by repeating experiments at least three times in triplicate.

Our data show that WhiB3 positively regulates the pH-specific expression of various genes involved in producing secretory proteins and lipids [*e.g.*, SL-1 (*pks2, papA1, mmpL8*), TDM (*fabD, acpP, kasA*), ESX-1 system (Rv3615c, Rv3870, Rv3871)] which are well known to restrict phagosomal maturation (27-29). Hence, the inability of *MtbΔwhiB3* to block phagosomal maturation could be a consequence of defective polyketide surface lipid anabolism. To investigate this, total surface exposed lipids were extracted from wt *Mtb* as described earlier (17). Moreover, pretreatment of macrophages with the surface exposed lipids of mycobacteria has been shown to modulate cellular processes such as phagosomal maturation and autophagy (30,31). Based on these studies, THP-1 cells were pretreated with the surface lipids and subsequently infected with wt *Mtb* or *MtbΔwhiB3* at a moi of 10. Infected macrophages were assessed for the colocalization of Lysotracker with *MtbΔwhiB3* at 0, and 24 h p.i.. Assessment of more than 100 phagosomes revealed that pretreatment with the wt *Mtb* lipids resulted in a significant inhibition of Lysotracker staining of *MtbΔwhiB3*-containing phagosomes as compared to untreated controls at each time point tested (Fig. 7A-C). Importantly, the percentage of Lysotracker-positive phagosomes containing *MtbΔwhiB3*upon pre-treatment with total lipids was comparable with wt *Mtb* at 0 h p.i. (Fig. 7A and C). These results suggest that the altered composition of surface-associated polyketide lipids is likely to be one of the factors responsible for the defective ability of *MtbΔwhiB3* to block phagosomal maturation. In sum, the data generated from macrophages and *in vitro* experiments clearly suggest that WhiB3 protects *Mtb* from acid stress by regulating gene expression, dynamic changes in E_{MSH} of *Mtb*, and polyketide-mediated restriction of phagosomal acidification.

WhiB3 modulates the expression of host innate response genes

We examined if WhiB3-mediated regulation of bioactive lipids and secretory proteins modulates expression of host transcriptome. Using microarrays, we compared the expression of THP-1 cells infected with wt *Mtb* and *MtbΔwhiB3* at various time points. We found that major innate immune mechanisms normally suppressed by pathogenic *Mtb* strains such as phagosomal maturation/endocytosis, apoptosis, and TLR

signaling were up-regulated in *MtbΔwhiB3* (1.5X, $p<0.05$), whereas genes which negatively regulate autophagy such as mTOR signaling were largely down-regulated in the mutant as compared to wt *Mtb* (1.5X, $p<0.05$) (Fig. 8, Table S2). In agreement with the role of WhiB3 in responding to early increase in phagosomal acidity, we observed a significantly greater impact of WhiB3 loss on host transcriptome at an early time point i.e. 12 h p.i. (Fig. 8). Finally, using qRT-PCR, we validated microarray data by measuring the expression of a selected set of genes involved in phagosomal maturation in a *whiB3*-dependent manner (data not shown). Altogether, data indicate that WhiB3 plays an important role in influencing expression of host-directed mechanisms associated with controlling intraphagosomal survival of *Mtb*.

WhiB3 regulates survival of *Mtb in vivo*

Given that WhiB3 regulates pH-dependent modulation of expression and redox signaling, resulting in differential intracellular trafficking and survival inside macrophages, we hypothesize that WhiB3 plays an important role during *Mtb* infection. To examine this, we assessed the *in vivo* phenotype of *MtbΔwhiB3* in guinea pigs. Aerosol infection of out-bred Hartley guinea pigs showed a clear growth attenuation of *MtbΔwhiB3* as compared to wt *Mtb* in the lungs of animals. At day 1 p.i., CFU analysis showed that nearly identical numbers of bacteria were implanted in the lungs of guinea pigs infected with wt *Mtb*, *MtbΔwhiB3*, and *whiB3-comp* strain (Fig. 9A). At day 30 and 60 p.i., the number of bacteria present in lungs of animals infected with *MtbΔwhiB3* was ~70 (p value=0.0073) and ~200-fold (p value= 0.0007) lower than those infected with wt *Mtb*, respectively (Fig. 9A). Interestingly, in contrast to our lung data, bacterial numbers in the spleen at day 30 and 60 p.i. were comparable in wt *Mtb* and *MtbΔwhiB3* (Fig. 9B). The attenuated virulence phenotype exhibited by *MtbΔwhiB3* was partially restored in the animals infected with *whiB3-comp* strain (Fig. 9A). Histopathological analysis of lungs from infected animals further validated the requirement of WhiB3 during infection. The lungs of *MtbΔwhiB3*-infected animals showed less severe pathology as indicated by decreased tissue consolidation, smaller granulomas, and open alveolar space as compared wt *Mtb* and *whiB3-comp* strain (Fig. 9C).

DISCUSSION

In 1905, Elie Metchnikoff reported the presence of acidic milieu within the phagosomes of macrophages infected with pathogens (32). Despite this early observation, how *Mtb* bacilli respond, resist, and persist in response to a gradient of acidic pH during infection remains poorly characterized. Here, we identified acidic pH as a physiological stimulus to which WhiB3 regulates: (i) gene expression, (ii) mycothiol redox homeostasis, (iii) phagosomal maturation, and (iv) virulence.

Our microarray data highlight the role of WhiB3 in regulating acid stress response in *Mtb*. Differential regulation of several genes involved in redox metabolism of *Mtb* in response to acid stress in a WhiB3-dependent manner, and acute sensitivity displayed by *MtbΔwhiB3* at pH 4.5, suggest that WhiB3 facilitates *Mtb* persistence in response to acid stress by maintaining intramycobacterial redox homeostasis. Until now, direct evidence linking acidic stress encountered in phagosomes to internal redox balance of *Mtb* was lacking. A recent *in vitro* study, using a genetically encoded redox biosensor (roGFP-R12), has demonstrated that the cytoplasmic redox state of *Mtb* shifts to reductive when bacilli were cultured under specific carbon sources at pH 5.5 (33). Since conventional roGFPs such as roGFP-R12 predominantly interact with glutathione redox buffer(34, 35), which is absent in mycobacteria, the utility of roGFPs in *Mtb* is limited by unknown specificity and poor response to changes in redox potential (15). Moreover, reliable measurement range for roGFPs (*i.e.,* between 10-90% of sensor oxidation) covers about ±30 mV from the standard mid-point potential (34). Therefore, roGFP-R12 with a less negative mid-point potential (-265 mV) cannot accurately measure a reductive shift in

redox potential beyond -295 mV. In this context, Mrx1-roGFP2 with a mid-point potential of -280 mV allowed dynamic and precise imaging of the E_{MSH} of *Mtb*, in response to both oxidative and reductive stresses, with high sensitivity and temporal resolution (15, 36). Using this bio-probe, we provide an accurate numerical evidence that acidic pH promotes reductive shift in E_{MSH} of *Mtb in vitro* and inside phagosomes in a WhiB3-dependent manner. The reductive shift in E_{MSH} at initial phases of intramacrophage growth is consistent with the rapid drop in vacuolar pH within minutes of infection with *Mtb* (24), which also serves as an early cue to induce expression of genes linked to reductive stress (*e.g.,whiB3, whiB7,* and *dosR*) (29, 37). Moreimportantly, inhibition of vacuolar acidification resulted in both the loss of gene expression (28) and a substantial decrease in the *Mtb* subpopulations with E_{MSH}-reduced.

In contrast to wt *Mtb*, which preferentially resides in early endosomes, we observed that *MtbΔwhiB3*mainly localized to acidified lysosomes and displayed higher proportion of E_{MSH}-oxidized bacilli. These findings support our earlier observations that lysosomes enrich E_{MSH}-oxidized bacteria, whereas phagosomes with limited acidity (early endosomes) induce a reductive shift in E_{MSH} of *Mtb* (15). Interestingly, while treatment with BafA1 prevented acidification of *MtbΔwhiB3*-containing phagosomes and reversed intramacrophage survival defect, the proportion of mutant bacilli with E_{MSH}-oxidized remained uninfluenced. One likely possibility is that the loss of WhiB3 compromised the ability of the mutant to respond to changes in the phagosomal environment via mycothiol redox system. In line with this, several components of mycothiol pathway, including MSH disulfide reductase (Mtr) involved in recycling MSSM to MSH, are down-regulated in *MtbΔwhiB3* upon acid stress. Alternatively, *MtbΔwhiB3* may exploit another antioxidant system such as ergothionine (ERG) to respond to intraphagosomal environment. A compensatory protective role of ERG has already been established in mycothiol defective mycobacterial strains (38). Since Mrx1-roGFP2 does not respond to ERG (15), further work testing the role of ERG redox potential will allow more precise determination of relative contributions of ERG and MSH pathways in responding to phagosomal milieu.

The acidic pH-induced reductive E_{MSH} in wt *Mtb* most likely resulted from increased synthesis of MSH or higher rate of MSSM reduction to MSH via the activity of NADPH-dependent Mtr enzyme. Expression data indicated a significant up-regulation of MSH-biosynthetic genes in response to acidic pH. Additionally, a decreased expression of respiratory genes involved in regenerating NAD^+cofactor (*e.g.,* nuo operon), along with the up-regulation of fatty acid catabolic genes which generate excessive NADH through β-oxidation, may further lead to accumulation of NADH/NADPH cofactors during acidity. Because excessive accumulation of NADH/NADPH is known to elevate endogenous ROS levels through auto-oxidation or via Fenton reaction (39, 40), a reductive shift in E_{MSH} by NADPH-dependent conversion of MSSM to MSH via Mtr could be a mechanism to dispose off excess reductants. In this context, studies in *Mtb* have indicated only a marginal increase in NADPH pool at acidic pH, while levels of cytoplasmic thiols such as MSH and CoA-SH were substantially elevated (33, 41), agreeing with our findings that MSH pathway can function as a reductive sink to reduce toxicity associated with low pH. Further strengthening this connection is our finding showing inability of *MtbΔwhiB3* to maintain E_{MSH}-reduced, along with a previous report demonstrating massive accumulation of NADH/NADPH in *MtbΔwhiB3* inside macrophages (17). The mycothiol redox system has recently been shown to interact with a major antioxidant enzyme; superoxide dismutase, to exert an efficient adaptive response during infection (42). In light of this, an early elevation in reductive capacity of mycothiol (E_{MSH}-reduced), in response to vacuolar pH, might be important to activate additional mechanisms to detoxify a range of hostile radicals *Mtb* encounters later in the infection cycle (*e.g.* during immune-activation). Altogether, these observations, and the fact that external acidity does not increase H^+ concentration inside *Mtb* (10), serve to implicate intrabacterial

reductive E_{MSH} as an internal physiological signal to which *Mtb* responds through WhiB3 to coordinate gene expression and survival. These findings were further strengthened by our data showing a complete loss of *whiB3* induction along with other pH responsive genes in *Mtb* strain lacking mycothiol (*MtbΔmshA)* at acidic pH. Since WhiB3 is cytoplasmically located and implicated in responding to changes in intracellular redox conditions through redox-sensitive [4Fe-4S] cluster (13, 17), we hypothesize that the intramycobacterial reductive E_{MSH} under acidic stress can promote accumulation and/or stabilization of reduced form of 4Fe-4S cluster ($[4Fe\text{-}4S]^{1+}$-WhiB3) which directly or indirectly activates pH-responsive genes in *Mtb*. Alternatively, since the DNA binding activity of apo-WhiB3 (without Fe-S cluster) is modulated by the redox state of its cysteine thiols(17), an interesting possibility is that the reversible S-mycothiolation of WhiB3 thiols in response to pH-mediated changes in E_{MSH}, may function as redox regulatory switch to modulate gene expression. The functional linkage between MSH and WhiB3, as revealed in this study, can now be exploited to understand the molecular mechanism(s) of how mycothiol exerts its influence on the redox behavior and gene regulatory properties of WhiB3.

We found that *MtbΔwhiB3* has impaired ability to arrest phagosomal maturation, which can be rescued by supplementation of surface associated polyketide lipids from wt *Mtb*. These discoveries have significant implications in understanding mycobacterial pathogenesis, which suggest an intertwined association between immuno-modulatory virulence factors with the core metabolic processes in *Mtb*. We propose that WhiB3-mediated synthesis of virulence factors, including secretory lipids and proteins (ESX-1 system), in response to intracellular redox changes associated with acidic pH will play a larger part, in both redox maintenance and in counteracting phagosomal acidification, to ensure long term persistence of *Mtb* (Fig. 10). While our results indicate WhiB3 as a major regulator of pH- and redox-homeostasis, other regulators such as PhoP, which similarly modulate the expression of virulence factors to influence phagosomal maturation and intraphagosomal survival, can provide overlapping control over pH- and redox-response in *Mtb* (33, 43). Finally, the physiological significance of our mechanistic findings comes from dramatic attenuation of *MtbΔwhiB3* in the lungs of guinea pigs. Our results are in complete contrast with the previous findings of *MtbΔwhiB3* phenotype *in vivo* in mice (11, 44). Considering that guinea pigs are more relevant model systems for recapitulating human TB pathology, and the fact that hypoxic caseous TB granulomas formed in lungs of guinea pigs can expose *Mtb* to more acidic environment (45), might have necessitated the need of WhiB3-dependent redox sensing pathway for ensuring redox homeostasis, survival and persistence of *Mtb in vivo*.

In summary, we have identified a new mechanism exploited by *Mtb* to respond to phagosomal pH. Our study provides a unique example of the tight connections forged between core redox machinery and virulence in mycobacterial pathogenesis. Furthermore, pH-induced redox changes and its connection with gene expression and virulence may be relevant to other intracellular pathogens. For example, acidification is required for virulence expression in *Salmonella* (46), phagosomal escape of *Listeria monocytogenes* (47), and efficient replication of *Legionella pneumophilla* and *Coxiella burnetti* (48, 49). Thus our findings have broad implications on several of intracellular pathogens where phagosomal pH plays a critical role in modulating virulence and long term persistence.

ACKNOWLEDGMENTS

We are thankful to the University of Delhi South Campus MicroArray Centre (UDSCMAC), New Delhi, and Bionivid Technologies Pv, Ltd, Bangalore, for conducting microarray experiments. We also thank DBT- India for supporting BSL3 Facilities (TACF) at ICGEB, New Delhi, and IISc, Bangalore. We thank

Pankti Parikh for assistance in generating *MtbΔwhiB3* strain and MohamedHusen Munshi for lipid isolation from *Mtb*. We are also grateful to Mr. Manish Kumar and Dr. Sheetal Gandotra, present in-charge of Imaging Facility at CSIR-Institute of Genomics and Integrative Biology, New Delhi, for an extensive technical help with all the confocal microscopy experiments and analysis.

CONFLICT OF INTEREST

The authors declare that they have no conflicts of interest with the contents of this article.

AUTHOR CONTRIBUTIONS

MM and AS designed research; MM and RSR performed research; and MM and AS wrote the paper. All authors analyzed the results and approved the final version of the manuscript.

REFERENCES

1. Ehrt, S., and Schnappinger, D. (2009) Mycobacterial survival strategies in the phagosome: defence against host stresses. *Cellular microbiology* **11**, 1170-1178
2. Schnappinger, D., Ehrt, S., Voskuil, M. I., Liu, Y., Mangan, J. A., Monahan, I. M., Dolganov, G., Efron, B., Butcher, P. D., Nathan, C., and Schoolnik, G. K. (2003) Transcriptional Adaptation of *Mycobacterium tuberculosis* within Macrophages: Insights into the Phagosomal Environment. *The Journal of experimental medicine* **198**, 693-704
3. Rohde, K. H., Veiga, D. F., Caldwell, S., Balazsi, G., and Russell, D. G. (2012) Linking the transcriptional profiles and the physiological states of *Mycobacterium tuberculosis* during an extended intracellular infection. *PLoS pathogens* **8**, e1002769
4. Armstrong, J. A., and Hart, P. D. (1971) Response of cultured macrophages to *Mycobacterium tuberculosis*, with observations on fusion of lysosomes with phagosomes. *The Journal of experimental medicine* **134**, 713-740
5. Hart, P. D., and Armstrong, J. A. (1974) Strain virulence and the lysosomal response in macrophages infected with *Mycobacterium tuberculosis*. *Infection and immunity* **10**, 742-746
6. MacMicking, J. D., Taylor, G. A., and McKinney, J. D. (2003) Immune control of tuberculosis by IFN-gamma-inducible LRG-47. *Science* **302**, 654-659
7. Schaible, U. E., Sturgill-Koszycki, S., Schlesinger, P. H., and Russell, D. G. (1998) Cytokine activation leads to acidification and increases maturation of *Mycobacterium avium*-containing phagosomes in murine macrophages. *J Immunol* **160**, 1290-1296
8. Via, L. E., Fratti, R. A., McFalone, M., Pagan-Ramos, E., Deretic, D., and Deretic, V. (1998) Effects of cytokines on mycobacterial phagosome maturation. *Journal of cell science* **111 (Pt 7)**, 897-905
9. Vandal, O. H., Nathan, C. F., and Ehrt, S. (2009) Acid resistance in *Mycobacterium tuberculosis*. *Journal of bacteriology* **191**, 4714-4721
10. Vandal, O. H., Pierini, L. M., Schnappinger, D., Nathan, C. F., and Ehrt, S. (2008) A membrane protein preserves intrabacterial pH in intraphagosomal *Mycobacterium tuberculosis*. *Nature medicine* **14**, 849-854
11. Banaiee, N., Jacobs, W. R., Jr., and Ernst, J. D. (2006) Regulation of *Mycobacterium tuberculosis* whiB3 in the mouse lung and macrophages. *Infection and immunity* **74**, 6449-6457

12. Rohde, K. H., Abramovitch, R. B., and Russell, D. G. (2007) *Mycobacterium tuberculosis* invasion of macrophages: linking bacterial gene expression to environmental cues. *Cell host & microbe* **2**, 352-364
13. Singh, A., Guidry, L., Narasimhulu, K. V., Mai, D., Trombley, J., Redding, K. E., Giles, G. I., Lancaster, J. R., Jr., and Steyn, A. J. (2007) *Mycobacterium tuberculosis* WhiB3 responds to O2 and nitric oxide via its [4Fe-4S] cluster and is essential for nutrient starvation survival. *Proceedings of the National Academy of Sciences of the United States of America* **104**, 11562-11567
14. Singh, A., Jain, S., Gupta, S., Das, T., and Tyagi, A. K. (2003) mymA operon of *Mycobacterium tuberculosis*: its regulation and importance in the cell envelope. *FEMS microbiology letters* **227**, 53-63
15. Bhaskar, A., Chawla, M., Mehta, M., Parikh, P., Chandra, P., Bhave, D., Kumar, D., Carroll, K. S., and Singh, A. (2014) Reengineering redox sensitive GFP to measure mycothiol redox potential of *Mycobacterium tuberculosis* during infection. *PLoS pathogens* **10**, e1003902
16. Venkataraman, B., Vasudevan, M., and Gupta, A. (2014) A new microarray platform for whole-genome expression profiling of *Mycobacterium tuberculosis*. *Journal of microbiological methods* **97**, 34-43
17. Singh, A., Crossman, D. K., Mai, D., Guidry, L., Voskuil, M. I., Renfrow, M. B., and Steyn, A. J. (2009) *Mycobacterium tuberculosis* WhiB3 maintains redox homeostasis by regulating virulence lipid anabolism to modulate macrophage response. *PLoS pathogens* **5**, e1000545
18. Hostetter, J. M., Steadham, E. M., Haynes, J. S., Bailey, T. B., and Cheville, N. F. (2002) Cytokine effects on maturation of the phagosomes containing Mycobacteria avium subspecies paratuberculosis in J774 cells. *FEMS immunology and medical microbiology* **34**, 127-134
19. Karim, A. F., Chandra, P., Chopra, A., Siddiqui, Z., Bhaskar, A., Singh, A., and Kumar, D. (2011) Express path analysis identifies a tyrosine kinase Src-centric network regulating divergent host responses to *Mycobacterium tuberculosis* infection. *The Journal of biological chemistry* **286**, 40307-40319
20. Rao, M., Streur, T. L., Aldwell, F. E., and Cook, G. M. (2001) Intracellular pH regulation by *Mycobacterium smegmatis* and Mycobacterium bovis BCG. *Microbiology* **147**, 1017-1024
21. MacMicking, J., Xie, Q. W., and Nathan, C. (1997) Nitric oxide and macrophage function. *Annual review of immunology* **15**, 323-350
22. Wong, D., Bach, H., Sun, J., Hmama, Z., and Av-Gay, Y. (2011) *Mycobacterium tuberculosis* protein tyrosine phosphatase (PtpA) excludes host vacuolar-H+-ATPase to inhibit phagosome acidification. *Proceedings of the National Academy of Sciences of the United States of America* **108**, 19371-19376
23. Sullivan, J. T., Young, E. F., McCann, J. R., and Braunstein, M. (2012) The *Mycobacterium tuberculosis* SecA2 system subverts phagosome maturation to promote growth in macrophages. *Infection and immunity* **80**, 996-1006
24. Sturgill-Koszycki, S., Schlesinger, P. H., Chakraborty, P., Haddix, P. L., Collins, H. L., Fok, A. K., Allen, R. D., Gluck, S. L., Heuser, J., and Russell, D. G. (1994) Lack of acidification in Mycobacterium phagosomes produced by exclusion of the vesicular proton-ATPase. *Science* **263**, 678-681
25. Singh, C. R., Moulton, R. A., Armitige, L. Y., Bidani, A., Snuggs, M., Dhandayuthapani, S., Hunter, R. L., and Jagannath, C. (2006) Processing and presentation of a mycobacterial antigen 85B epitope by murine macrophages is dependent on the phagosomal acquisition of vacuolar proton ATPase and in situ activation of cathepsin D. *J Immunol* **177**, 3250-3259

26. Clemens, D. L., and Horwitz, M. A. (1995) Characterization of the *Mycobacterium tuberculosis* phagosome and evidence that phagosomal maturation is inhibited. *The Journal of experimental medicine* **181**, 257-270
27. Brodin, P., Poquet, Y., Levillain, F., Peguillet, I., Larrouy-Maumus, G., Gilleron, M., Ewann, F., Christophe, T., Fenistein, D., Jang, J., Jang, M. S., Park, S. J., Rauzier, J., Carralot, J. P., Shrimpton, R., Genovesio, A., Gonzalo-Asensio, J. A., Puzo, G., Martin, C., Brosch, R., Stewart, G. R., Gicquel, B., and Neyrolles, O. (2010) High content phenotypic cell-based visual screen identifies *Mycobacterium tuberculosis* acyltrehalose-containing glycolipids involved in phagosome remodeling. *PLoS pathogens* **6**, e1001100
28. MacGurn, J. A., and Cox, J. S. (2007) A genetic screen for *Mycobacterium tuberculosis* mutants defective for phagosome maturation arrest identifies components of the ESX-1 secretion system. *Infection and immunity* **75**, 2668-2678
29. Pethe, K., Swenson, D. L., Alonso, S., Anderson, J., Wang, C., and Russell, D. G. (2004) Isolation of *Mycobacterium tuberculosis* mutants defective in the arrest of phagosome maturation. *Proceedings of the National Academy of Sciences of the United States of America* **101**, 13642-13647
30. Zullo, A. J., and Lee, S. (2012) Mycobacterial induction of autophagy varies by species and occurs independently of mammalian target of rapamycin inhibition. *The Journal of biological chemistry* **287**, 12668-12678
31. Axelrod, S., Oschkinat, H., Enders, J., Schlegel, B., Brinkmann, V., Kaufmann, S. H., Haas, A., and Schaible, U. E. (2008) Delay of phagosome maturation by a mycobacterial lipid is reversed by nitric oxide. *Cellular microbiology* **10**, 1530-1545
32. Metchnikoff, E. (1905) *Immunity to infective disease*, Cambridge University Press, Cambridge, United Kingdom
33. Baker, J. J., Johnson, B. K., and Abramovitch, R. B. (2014) Slow growth of *Mycobacterium tuberculosis* at acidic pH is regulated by phoPR and host-associated carbon sources. *Molecular microbiology* **94**, 56-69
34. Meyer, A. J., and Dick, T. P. (2010) Fluorescent protein-based redox probes. *Antioxidants & redox signaling* **13**, 621-650
35. Bhaskar, A., Munshi, M., Khan, S. Z., Fatima, S., Arya, R., Jameel, S., and Singh, A. (2015) Measuring glutathione redox potential of HIV-1-infected macrophages. *The Journal of biological chemistry* **290**, 1020-1038
36. Tyagi, P., Dharmaraja, A. T., Bhaskar, A., Chakrapani, H., and Singh, A. (2015) *Mycobacterium tuberculosis* has diminished capacity to counteract redox stress induced by elevated levels of endogenous superoxide. *Free radical biology & medicine* **84**, 344-354
37. Geiman, D. E., Raghunand, T. R., Agarwal, N., and Bishai, W. R. (2006) Differential gene expression in response to exposure to antimycobacterial agents and other stress conditions among seven *Mycobacterium tuberculosis* whiB-like genes. *Antimicrobial agents and chemotherapy* **50**, 2836-2841
38. Ta, P., Buchmeier, N., Newton, G. L., Rawat, M., and Fahey, R. C. (2011) Organic hydroperoxide resistance protein and ergothioneine compensate for loss of mycothiol in *Mycobacterium smegmatis* mutants. *Journal of bacteriology* **193**, 1981-1990
39. Yan, L. J., Levine, R. L., and Sohal, R. S. (1997) Oxidative damage during aging targets mitochondrial aconitase. *Proceedings of the National Academy of Sciences of the United States of America* **94**, 11168-11172
40. Woodmansee, A. N., and Imlay, J. A. (2003) A mechanism by which nitric oxide accelerates the rate of oxidative DNA damage in Escherichia coli. *Molecular microbiology* **49**, 11-22

41. Buchmeier, N. A., Newton, G. L., and Fahey, R. C. (2006) A mycothiol synthase mutant of *Mycobacterium tuberculosis* has an altered thiol-disulfide content and limited tolerance to stress. *Journal of bacteriology* **188**, 6245-6252
42. Nambi, S., Long, J. E., Mishra, B. B., Baker, R., Murphy, K. C., Olive, A. J., Nguyen, H. P., Shaffer, S. A., and Sassetti, C. M. (2015) The Oxidative Stress Network of *Mycobacterium tuberculosis* Reveals Coordination between Radical Detoxification Systems. *Cell host & microbe* **17**, 829-837
43. Ferrer, N. L., Gomez, A. B., Neyrolles, O., Gicquel, B., and Martin, C. (2010) Interactions of attenuated *Mycobacterium tuberculosis* phoP mutant with human macrophages. *PloS one* **5**, e12978
44. Steyn, A. J., Collins, D. M., Hondalus, M. K., Jacobs, W. R., Jr., Kawakami, R. P., and Bloom, B. R. (2002) *Mycobacterium tuberculosis* WhiB3 interacts with RpoV to affect host survival but is dispensable for in vivo growth. *Proceedings of the National Academy of Sciences of the United States of America* **99**, 3147-3152
45. Via, L. E., Lin, P. L., Ray, S. M., Carrillo, J., Allen, S. S., Eum, S. Y., Taylor, K., Klein, E., Manjunatha, U., Gonzales, J., Lee, E. G., Park, S. K., Raleigh, J. A., Cho, S. N., McMurray, D. N., Flynn, J. L., and Barry, C. E., 3rd. (2008) Tuberculous granulomas are hypoxic in guinea pigs, rabbits, and nonhuman primates. *Infection and immunity* **76**, 2333-2340
46. Helaine, S., Cheverton, A. M., Watson, K. G., Faure, L. M., Matthews, S. A., and Holden, D. W. (2014) Internalization of *Salmonella* by macrophages induces formation of nonreplicating persisters. *Science* **343**, 204-208
47. Beauregard, K. E., Lee, K. D., Collier, R. J., and Swanson, J. A. (1997) pH-dependent perforation of macrophage phagosomes by listeriolysin O from *Listeria monocytogenes*. *The Journal of experimental medicine* **186**, 1159-1163
48. Maurin, M., Benoliel, A. M., Bongrand, P., and Raoult, D. (1992) Phagolysosomes of *Coxiella burnetii*-infected cell lines maintain an acidic pH during persistent infection. *Infection and immunity* **60**, 5013-5016
49. Sturgill-Koszycki, S., and Swanson, M. S. (2000) *Legionella pneumophila* replication vacuoles mature into acidic, endocytic organelles. *The Journal of experimental medicine* **192**, 1261-1272

FOOTNOTES:

We thank the Department of Biotechnology (DBT), Ministry of Science and Technology, India BT/PR5020/MED/29/454/2012, BT/03/IYBA/2010 [AS]) and Wellcome-DBT India Alliance (500034/Z/09/Z [AS]) for financial support. AS acknowledges DBT-Innovative Young Biotechnologist Award (IYBA). AS is a fellow of Wellcome-DBT India Alliance. MM acknowledges a fellowship from Council for Scientific and Industrial Research (CSIR). The abbreviations used were: ADS, Albumin-Dextrose-Saline; MES, 2-(4-morpholino)-ethane sulfonic acid; BafA1, Bafilomycin A1; CCCP, Carbonyl cyanide m-chlorophenylhydrazone; CFUs, Colony-forming units; CcA, Concanamycin A; DAT, diacyltrehalose;E_{MSH}, Mycothiol redox potential; ERG, Ergothionine; FITC, Fluorescein 5(6)-isothiocyanate; GEO, Gene Expression Omnibus; H^+ V-ATPase ,vacuolar H^+-ATPase; IFN-γ, Interferon-gamma; LAMP-1, Lysosomal associated marker protein-1, LF, Left flanking regions; LPS , Lipopolysaccharide; Mrx1, Mycoredoxin; MSH, Mycothiol; Mtr, MSH disulfide reductase; MOI, Multiplicity of infection; *Mtb*, *Mycobacterium tuberculosis*; NEM, N-Ethylmaleimide; NO, Nitric oxide; ORF, open reading frame; PAT, polyacyltrehalose; PBS, phosphate buffer saline; PFA, paraformaldehyde; ΔpH , pH gradient; PMA, Phorbol 12-myristate 13-acetate; qRT-PCR , Quantitative RT-PCR; RF, Right flanking regions; roGFP, Redox-sensitive green fluorescent protein; ROS, Reactive

oxygen species;RNS, Reactive nitrogen species; RT, Room temperature; SD, standard deviation; SL-1, sulfolipid-1; TAG- Triacylglycerol; UDSCMAC, University of Delhi South Campus MicroArray Centre.

FIGURE LEGENDS

Figure 1: WhiB3 modulates survival of *Mtb* at acidic pH.

(A) Schematic representation of disrupted *whiB3* allele (*Rv 3416*) in the genome of *Mtb*. Entire *whiB3* ORF was replaced by 1-kb right and 1-kb left flanking regions of *whiB3* along with loxP-*hyg-gfp*-loxP cassette. (B) Genomic DNA was isolated from putative $Kan^{S}Hyg^{R}GFP^{+}$ *MtbΔwhiB3* colonies (26, 30 and 34) and replacement of *whiB3* allele with Hyg-GFP cassette was confirmed using PCR with F1 and R1 primers (Table 1). An increase in amplicon size from 2.4 kb to 4.5 kb due to insertion of loxP-*hyg-gfp*-loxP cassette was observed in case of mutant clones, confirming the double crossover event. (C) RNA was isolated from logarithmically grown wt *Mtb* and the putative *MtbΔwhiB3* clones. qRT-PCR for *whiB3* was done using *whiB3* specific oligonucleotides (Table 1) and C_t values were plotted to assess the expression. (D) For assessing survival of *Mtb* strains at acidic pH, wt *Mtb*, *MtbΔwhiB3, whiB3-comp* strains were grown in 7H9-Ty media at the indicated pH values for 4 days at 37°C and survival was assessed by enumerating CFUs. Data shown is the average of two independent experiments done in triplicate. Error bars represent SDs from the mean. ** $p<0.01$ (as compared to wt*Mtb*) and + $p<0.05$ (as compared to *whiB3-comp*).

Figure 2: WhiB3 regulates gene expression in response to acidic pH *in vitro*.

Wt *Mtb* and *MtbΔwhiB3* strains were grown to an O.D. $_{600\ nm}$ ~ 0.3 and exposed to acidic pH of 4.5 for 2 h at 37°C. Total RNA was isolated and subjected to microarray analysis as described in *Experimental procedures*. (A) Genes with > 2-fold ($p<0.05$) up- or down- regulation by acid stress relative to neutral pH were classified in 14 classes based on the annotation given in TubercuList. Pie chart represents the relative fraction of various pathways affected by acid stress in wt *Mtb*. (B) Heat map comparing wt *Mtb* and *MtbΔwhiB3* genes induced or repressed significantly (> 2-fold, p-value<0.05*)* at pH 4.5 relative to neutral pH. (C) Heat map showing the overlap of genes differentially regulated in wt *Mtb* and *MtbΔwhiB3* by *in vitro* acid stress (pH 4.5) with concanamycin A (CcA)-sensitive phagosome-induced genes (12). Highlighted areas represent genes affected by phagosomal acidification in wt *Mtb* in a WhiB3-dependent manner at pH 4.5 *in vitro* (1.5-fold up- and down-regulated, p-value<0.05).

Figure 3: WhiB3 regulates dynamic changes in intramycobacterial E_{MSH} of *Mtb* in response acid stress.

Wt *Mtb*, *MtbΔwhiB3* and *whiB3-comp* strains expressing Mrx1-roGFP2 were grown in 7H9-Ty media at a pH of (A) 7.0, (B) 6.2, (C) 5.5, and (D) 4.5. At indicated time points, E_{MSH} of 30,000 bacterial cells was measured by flow cytometry as described in *Experimental procedures*. At 72 h post-incubation, 500 µM of CCCP was added to dissipate the pH gradient and intramycobacterial E_{MSH} was measured 4 h post-CCCP treatment (*i.e.* 76 h). **$p<0.01$, ***$p<0.005$ (as compared to wt *Mtb*), +$p<0.05$, ++$p<0.01$, +++$p<0.005$ (as compared to *whiB3-comp*). Viability of *wt Mtb*, *MtbΔwhiB3* and *whiB3-comp* upon CCCP treatment at pH 7.0 (E), pH 4.5 (F and G) for 4 h, as determined by enumerating CFUs. Data shown in each panel is the result of at least two independent experiments performed in triplicate. Error bars represent standard deviations from the mean. **$p<0.01$, ***$p<0.005$.

Figure 4: Regulation of intramycobacterial E_{MSH} and survival of *Mtb* in a WhiB3-dependent manner inside macrophages.

THP-1 cells were infected with Mrx1-roGFP2 expressing (A) wt *Mtb*, (B) *MtbΔwhiB3*, and (C) *whiB3-comp* strains at a moi of 10. At indicated time points, ~ 30,000 infected macrophages were analyzed by flow cytometry, intramycobacterial E_{MSH} was measured, and percentage of bacilli in each subpopulation was determined as described earlier (15). The percentage of bacilli in each subpopulation (E_{MSH}-oxidized, E_{MSH}-basal and E_{MSH}-reduced) was plotted as a bar graph as described earlier (15). The "0" h time point refers to time immediately after infection with *Mtb* strains for 6 h (4 h of internalization followed by 2 h of amikacin treatment to remove any extracellular bacilli). (D) THP-1 macrophages were infected with wt *Mtb*, *MtbΔwhiB3*, and *whiB3-comp* strains as described above and intramacrophage survival was monitored, by enumerating CFUs, at indicated time points. IFN-γ and LPS treated (activated) RAW 264.7 macrophages were infected with Mrx1-roGFP2 expressing (E) wt *Mtb*, (F) *MtbΔwhiB3*, and (G) *whiB3-comp* strains (moi:10). At indicated time points, intramycobacterial E_{MSH} of *Mtb* subpopulations was measured as described in the earlier panel. (H) Activated RAW 264.7 macrophages were infected with wt *Mtb*, *MtbΔwhiB3* and *whiB3-comp* strains (moi:2) and intramacrophage survival was monitored as described in the earlier panel. The data in all panels are representative of three independent experiments performed in quadruplicates. Error bars represent SDs from the mean. In experiments related to measurements of E_{MSH}; *p<0.05 (E_{MSH}-oxidized subpopulation of *MtbΔwhiB3* as compared to wt *Mtb*) and $^{+}$p<0.05 (E_{MSH}-oxidized subpopulation of *MtbΔwhiB3* as compared to *whiB3 Comp*). In intramacrophage survival experiments; **p<0.01, ***<0.005 (as compared to wt *Mtb*), ++p<0.01, +++p<0.005 (as compared to *whiB3-comp*).

Figure 5: Phagosomal-acidification modulatesE_{MSH} and survival of *Mtb* in a WhiB3- dependent manner.

(A and B) THP-1 cells treated with 10 nM BafA1 or vehicle control (DMSO) were infected with wt *Mtb*, *MtbΔwhiB3* and *whiB3-comp* strains (moi:10) and at indicated time points, 30,000 infected cells were analyzed by flow cytometry and relative distribution of *Mtb* subpopulations with varying intramycobacterial E_{MSH} was measured as described earlier (15). The data are represented as percentage of bacilli in each subpopulation ± SD. *p<0.05, ***p<0.005 (E_{MSH}-reduced subpopulation in BafA1 untreated as compared to BafA1 treated cells). (C) THP-1 cells treated with BafA1 or vehicle control (DMSO) were infected with wt *Mtb*, *MtbΔwhiB3* and *whiB3-comp* strains and intramacrophage survival at the indicated time points was monitored by enumerating CFU. The data in all panels are representative of three independent experiments performed in quadruplicates. Error bars represent SDs from the mean. ***p<0.005 (BafA1 treated *MtbΔwhiB3*-infected THP-1 macrophages as compared to untreated control).

Figure 6: *MtbΔwhiB3* is enriched in phagosomes positive for late endosomal/lysosomal markers inside THP-1 macrophages.

THP-1 cells were infected with FITC-labelled wt *Mtb*, *MtbΔwhiB3, whiB3-comp* strains (moi: 10). At 24 h p.i., cells were independently stained with (A) Lysotracker or immuno-fluorescent antibodies for markers of phagosome maturation, *i.e.*, (B) H^{+} V-ATPase and (C) CD63, as described in *Experimental procedures*. A representative of three independent experiments is shown. In the images, green indicates FITC-labelled bacteria, red indicates Lysotracker or H^{+} V-ATPase or CD63, differential interference contrast (DIC) indicates cell morphology, and the yellow indicates merged images of two signals (Merge I: FITC/phagosomal markers) and three signals (Merge II: FITC/phagosomal markers/DIC). The scale bar represents 5 μm. The bar graphs represent mean percentages of bacterium-containing phagosomes that stain positive for markers. The error bars represents SDs of three replicate wells, with each well having ~

100-200 phagosomes scored. *p<0.05, ***p<0.005 (as compared with wt *Mtb*) and +p< 0.05, +++p<0.005 (as compared with *whiB3-comp*).

Figure 7: Treatment with surface exposed lipids derived from wt *Mtb* reduced the enrichment of *Mtb*Δ*whiB3* in acidified phagosomes.

Total surface exposed lipids were extracted from wt *Mtb* and coated onto coverslips, followed by seeding of THP-1 cells as described in *Experimental procedures*. Lipid- pretreated macrophages were infected with FITC-labelled *Mtb*Δ*whiB3* (moi: 10). As a control, untreated THP-1 cells were infected with FITC-labelled wt *Mtb* and *Mtb*Δ*whiB3* (moi: 10). At (A) 0 h, (B) 24 h p.i., cells were stained with Lysotracker and analyzed by confocal microscopy. Representative microscopy images from at least three independent experiments for each time point are shown. In the images, green indicates FITC-labelled bacteria, red indicates Lysotracker, DIC indicates cell morphology, and the yellow indicates merged images of two signals (Merge I: FITC/phagosomal markers) and three signals (Merge II: FITC/phagosomal markers/DIC). The scale bar represents 5 μm. The C panel represents mean percentages of bacterium-containing phagosomes that stain positive for Lysotracker. The error bars represent SD of three replicate wells, with each well having >100 phagosomes scored. *p<0.05, ***p<0.005 (as compared with wt *Mtb*), +p<0.05, and ++p<0.01 (as compared with *whiB3-comp*).

Figure 8: Regulation of host transcriptome by *Mtb* WhiB3

PMA differentiated THP-1 cells were infected with wt *Mtb* and *MtbΔwhiB3*. At indicated time points, total RNA from THP-1 was isolated and transcriptomic analysis was done, as described in *Experimental procedures*. The figure shows heat map of major pathways differentially regulated in *MtbΔwhiB3* as compared to *Mtb*, >1.5 fold (p<0.05).

Figure 9: WhiB3 regulates survival of *Mtb in vivo*

Outbred Hartley guinea pigs (n=5) were given an aerosol challenge with wt *Mtb, MtbΔwhiB3* and *whiB3-comp* strainsand assessed for survival in (A) lungs and (B) spleen. Error bars represent the SD from the mean. Statistical significance for the pulmonic and splenic bacterial load was obtained by comparing different strains: *** p<0.001 (as compared to wt *Mtb*), ++ p<0.005 (as compared to *whiB3Comp*). (C) Hematoxylin and eosin stained lung sections (30 and 60 days p.i.) from guinea pigs infected with wt *Mtb*, *MtbΔwhiB3* and the *whiB3-comp* strains. The pathology sections show granulomas (G) and alveolar space (AS). All images were taken at 40X magnification.

Figure 10: Model depicting the role of E_{MSH} and WhiB3 in responding to acid stress during infection.

In resting macrophages, *Mtb* impairs phagosome maturation and preferentially resides in a mildly acidic environment. Activation with IFN-γ induces phagosomal-lysosomal fusion to elevate the levels of proton (pH 4.5), ROI, and RNI in the microenvironment. Despite these changes in external pH, the internal pH of *Mtb* remains close to neutral (pH 7.2). Importantly, these variations in phagosomal pH induce dynamic changes in the E_{MSH} of *Mtb*. Limited acidification inside resting macrophages induces a reductive shift in E_{MSH} of *Mtb* (~ -305 mV), whereas activation of macrophages induces oxidative shift (-240 mV). Pharmacological inhibition of phagosomal acidification by BafA1 neutralizes acidic pH to prevent reductive shift in E_{MSH} of *Mtb*. *Mtb* responds to phagosomal acidification with the help of a putative redox-sensitive transcription factor, WhiB3. WhiB3 can sense changes in intrabacterial E_{MSH} via its Fe-S cluster or cysteine thiols (S-mycothiolation) to modulate the expression of virulence genes involved in blocking phagosomal maturation (*e.g.,* polyketides, secretory antigens) and redox

homeostasis. Impaired ability of *MtbΔwhiB3* to maintain mycothiol balance and block phagosomal maturation, along with the survival defect *in vivo*, suggest a central role of WhiB3 in regulating mycobacterial persistence in response to acid stress. The exact mechanisms by which WhiB3 senses pH-induced changes in internal E_{MSH} via 4Fe-4S and/or cysteine thiols remain to be identified.

Table 1: List of oligonucleotides used in the study.

Target	Primer sequence
whiB3 RT F	5' AACGCAGACATCTGGAACTG 3'
whiB3 RT R	5' TAGGGCTCACCGACCTCTAA 3'
pks2 RT F	5' AAGTGTCTCCGAGGTGTATG 3'
pks2 RT R	5' CGAGTGAAGTGCAGATTACG 3'
pks3 RT F	5'GGCTGAGATTGACACTGAAC 3'
pks3 RT R	5'TACCCGACATTCCATACGAG 3'
papA1 RT F	5' ATCCGCTAAGTACGATGGTC 3'
papA1 RT R	5' ACCGATCTAATTGCCCTCAG 3'
Rv3616c RT F	5' GAGCAGAGCGTTCATCATCG 3'
Rv3616c RTR	5' CGAACCTAACCAGCCATCAC 3'
Rv2390c RT F	5' CCGGCGAGTTCAAAGATAAG 3'
Rv2390c RT R	5' TGAACATCAGGACCACTACC 3'
16S rRNA RT F	5' GCCGTAAACGGTGGGTACTA 3'
16S rRNA RT R	5' TGCATGTCAAACCCAGGTAA 3'
MtbΔwhiB3 clone check F1	5' GTGGCATCGAGAGCCTCTTCAC 3'
MtbΔwhiB3 clone check R1	5' GACGCGTTGATCCTGCTGCAC 3'

Table 2: qRT-PCR analysis of a select set of pH-specific genes regulated by WhiB3 and mycothiol under acidic stress (pH 4.5).

Gene	*wt Mtb* 4.5/ *wt Mtb* 6.6	*MtbΔwhiB3* 4.5/ *wt Mtb 6.6*	*wt Mtb* 4.5/ *MtbΔwhiB3* 4.5	*wt Mtb* 7.0/ *MtbΔmshA* 7.0	*MtbΔmshA* 4.5/*MtbΔmshA* 7.0
whiB3	26±1.6	ND	ND	-1.1±0.47	-37.63±13.11
pks2	12±0.8	1.5±0.24	2±0.31	-1.66±0.805	-4.9±1.91
pks3	5.17±2.8	0.55±.0.16	9.3±0.62	-1.15±0.17	-5.11±2.46
papA1	4.6±2.25	0.71±0.07	6.1±0.53	-0.2±1.93	-12.43±4.76
Rv3616c	14.8±4.1	2.3±1	8±0.52	-1.46±2.48	1.96±0.26
Rv2390c	54±26	14.6±3.1	3.7±0.53	1.19±0.36	3.03±0.75

Expression is compared within various treatment groups and data is represented as fold-change in gene expression ± SD. ND: Not determined.

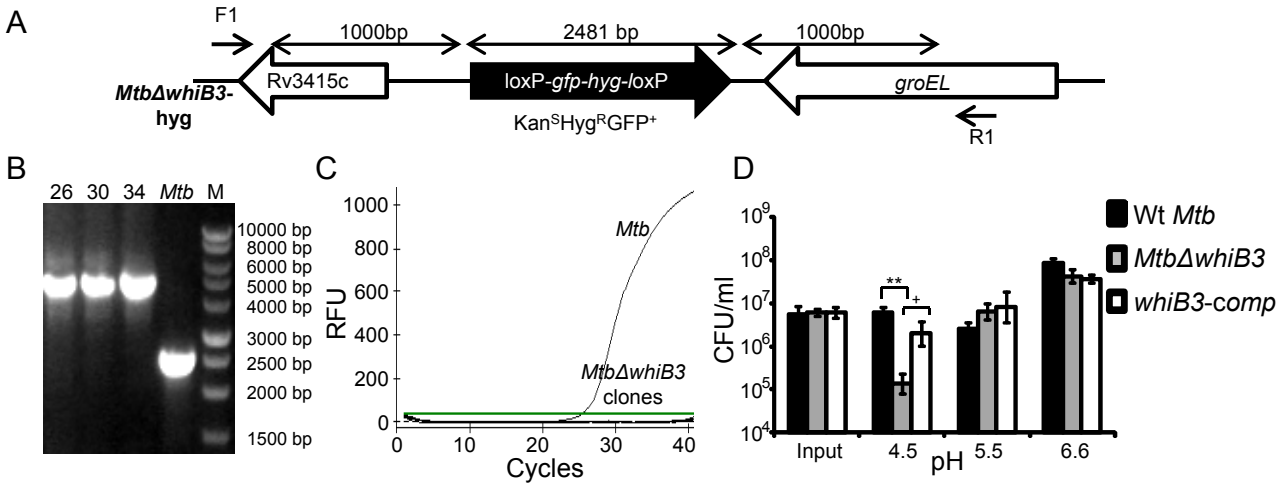

Fig. 1

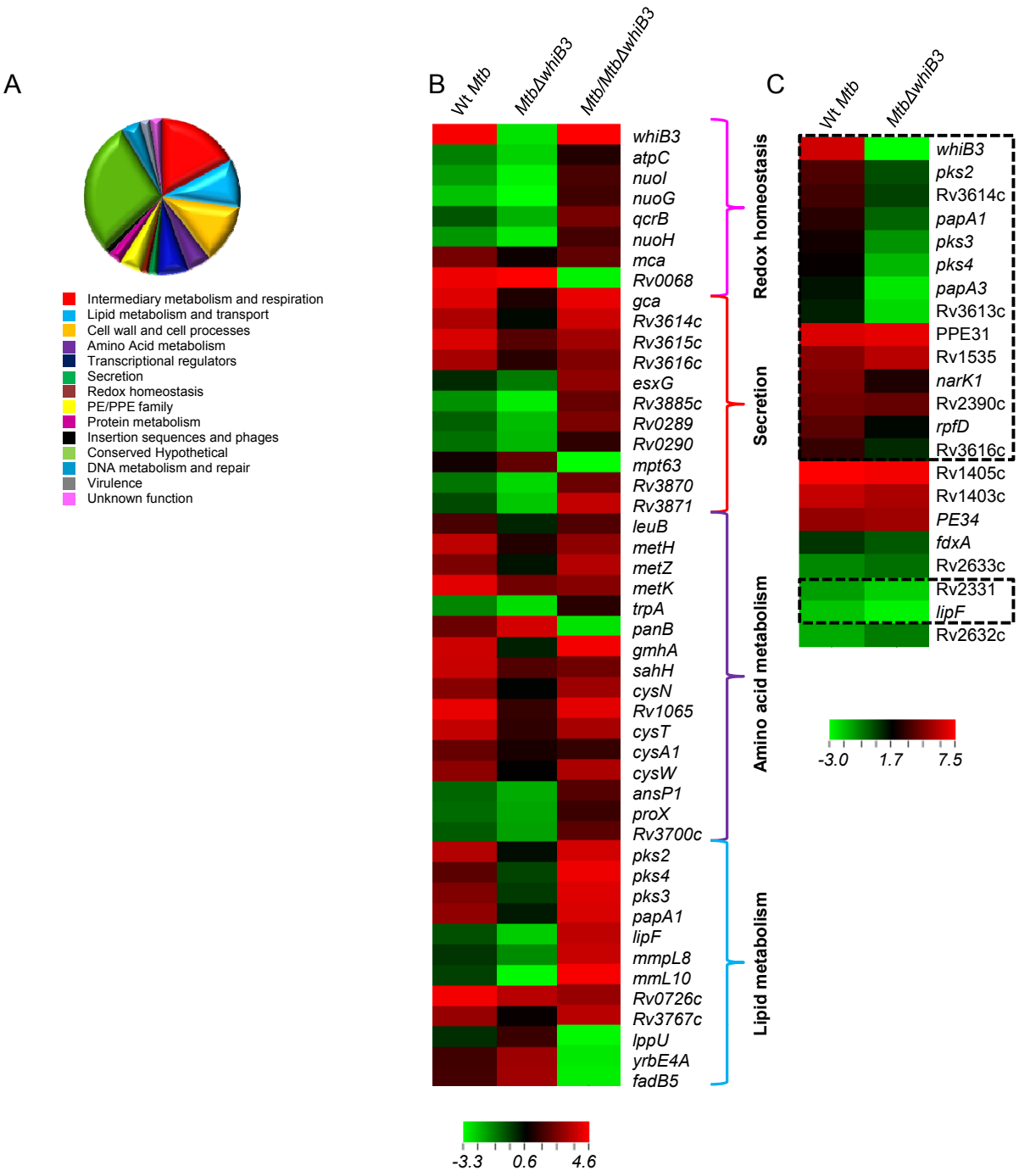

Fig. 2

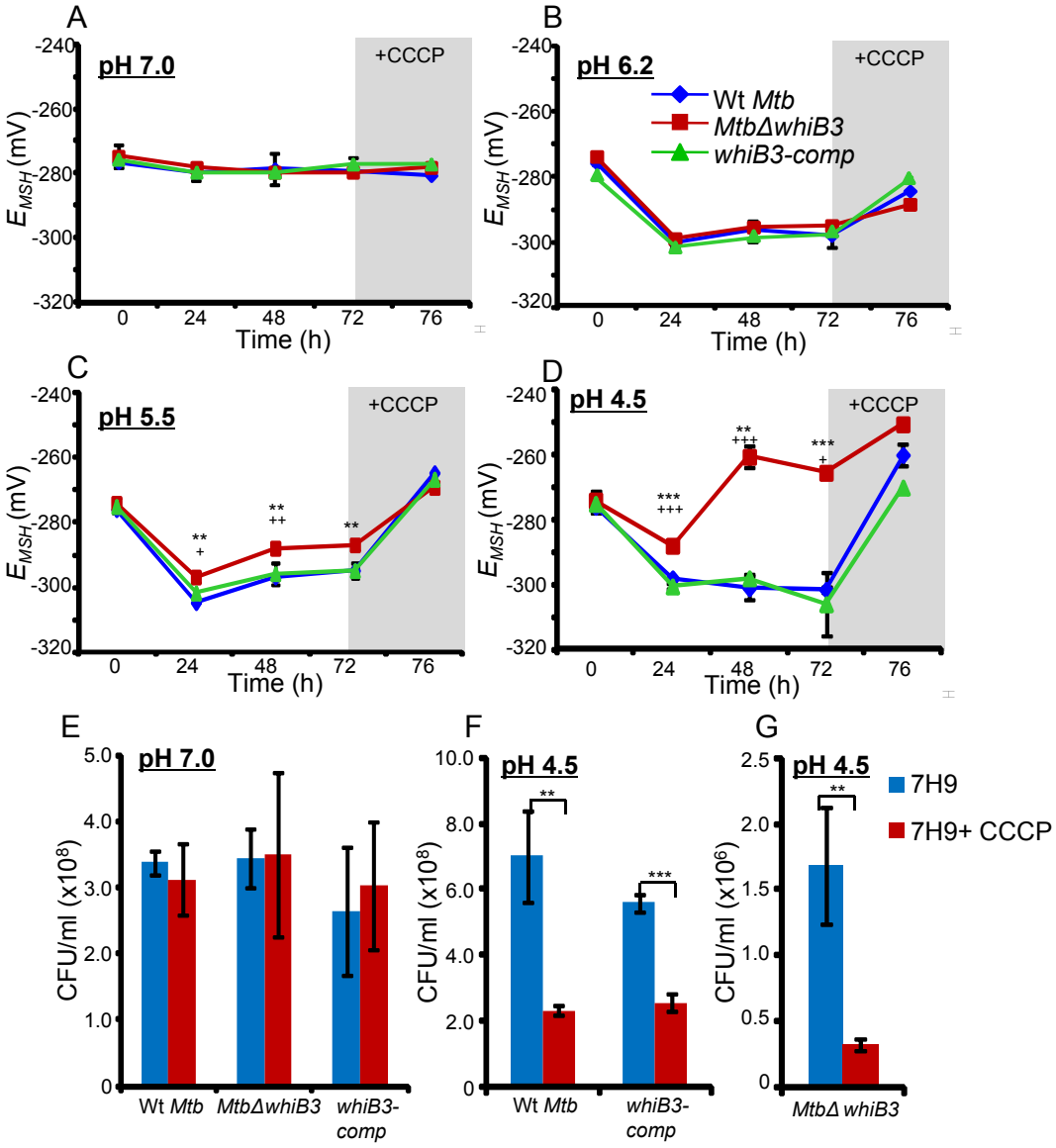

Fig. 3

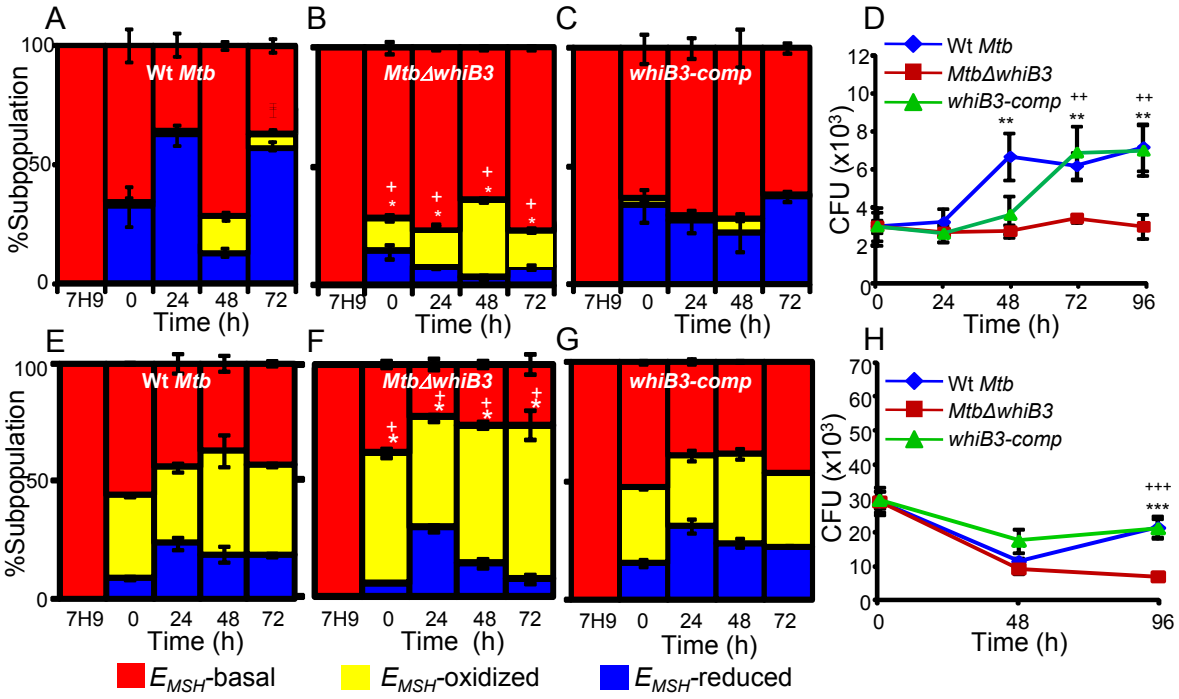

Fig. 4

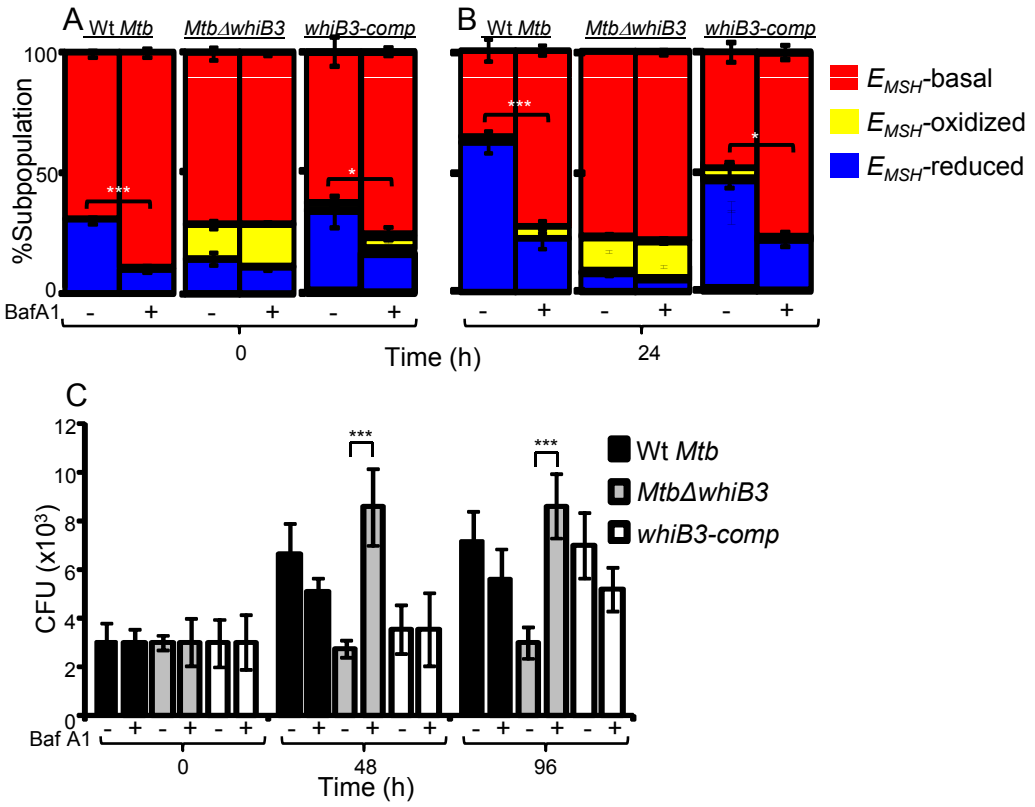

Fig. 5

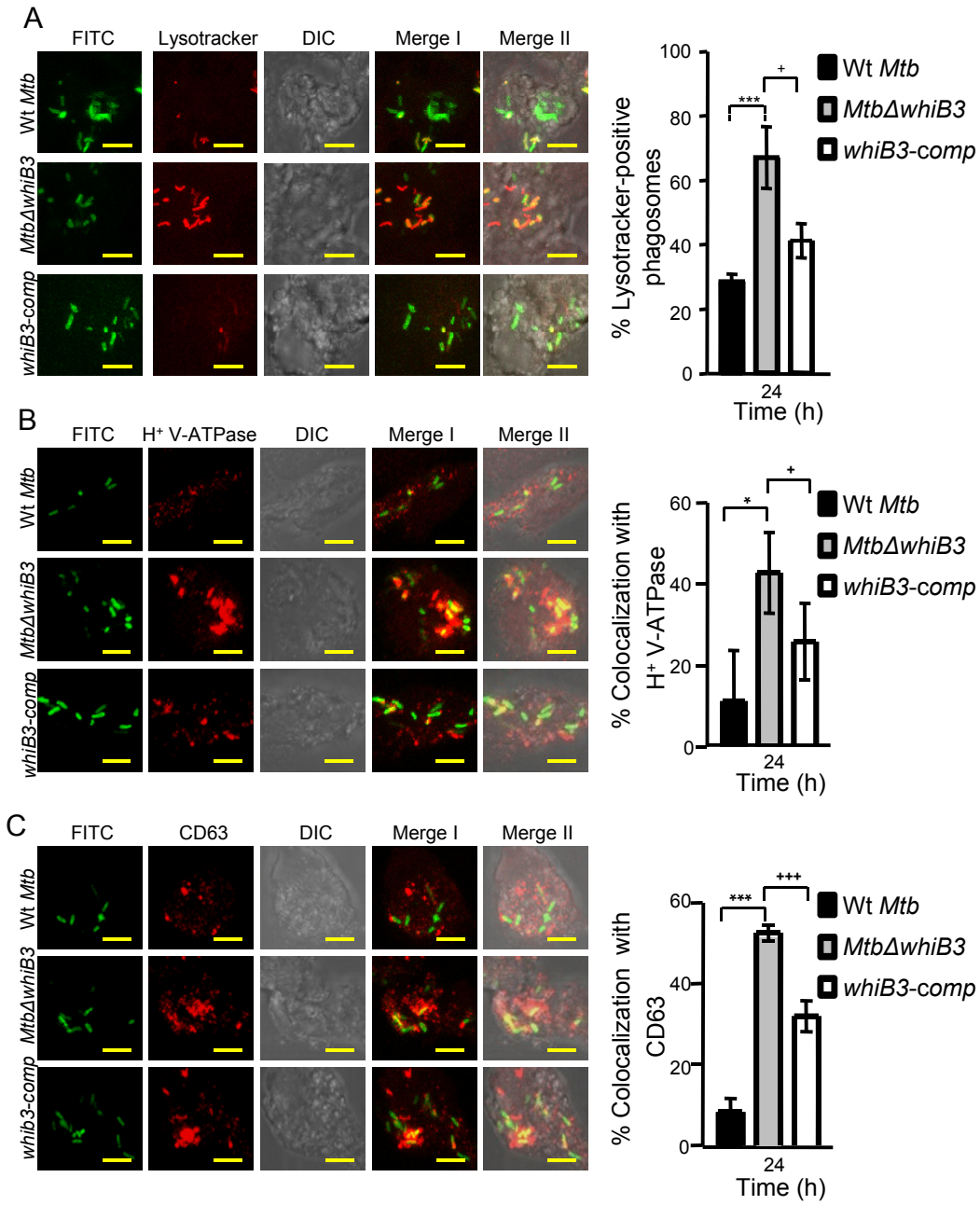

Fig. 6

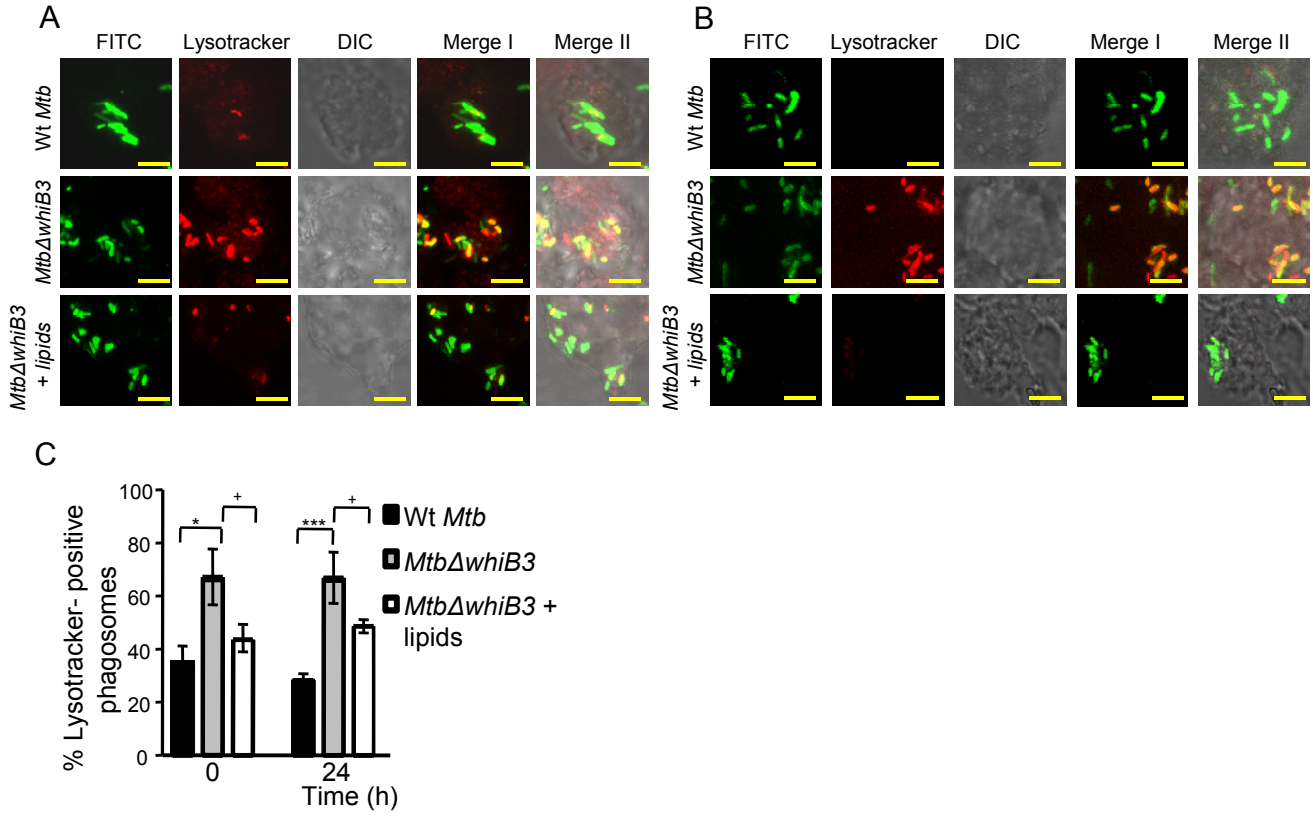

Fig. 7

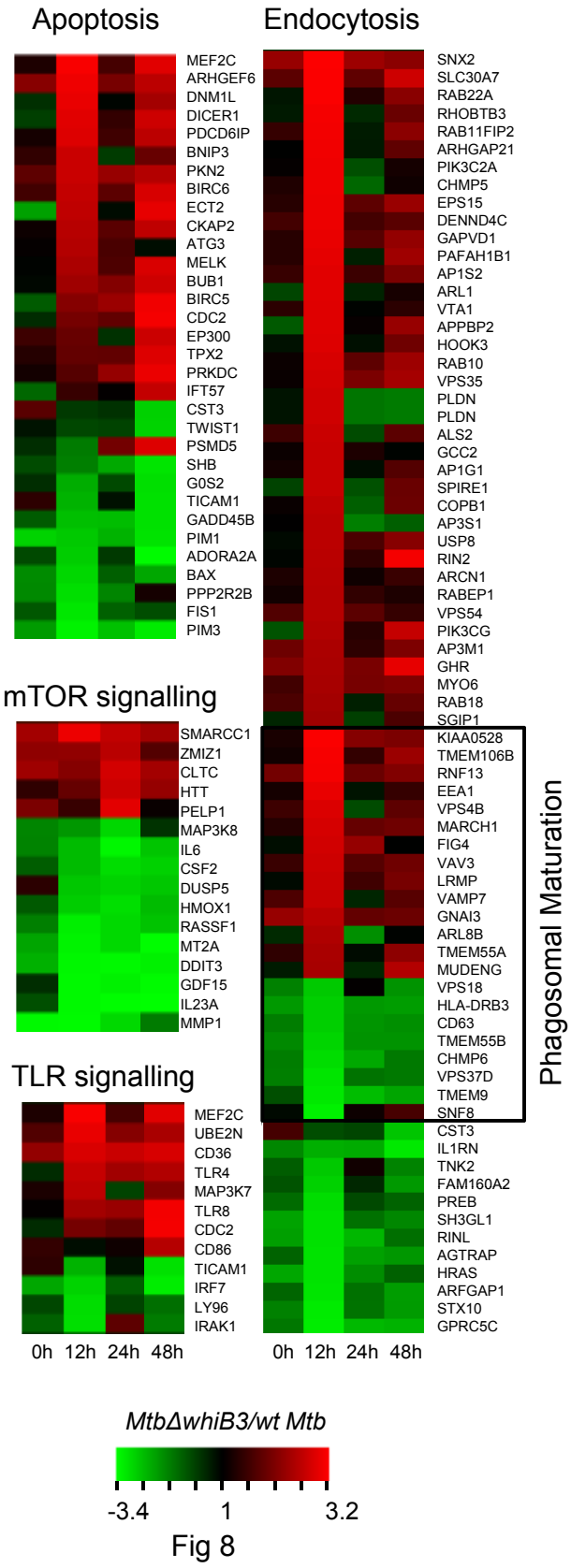

Fig 8

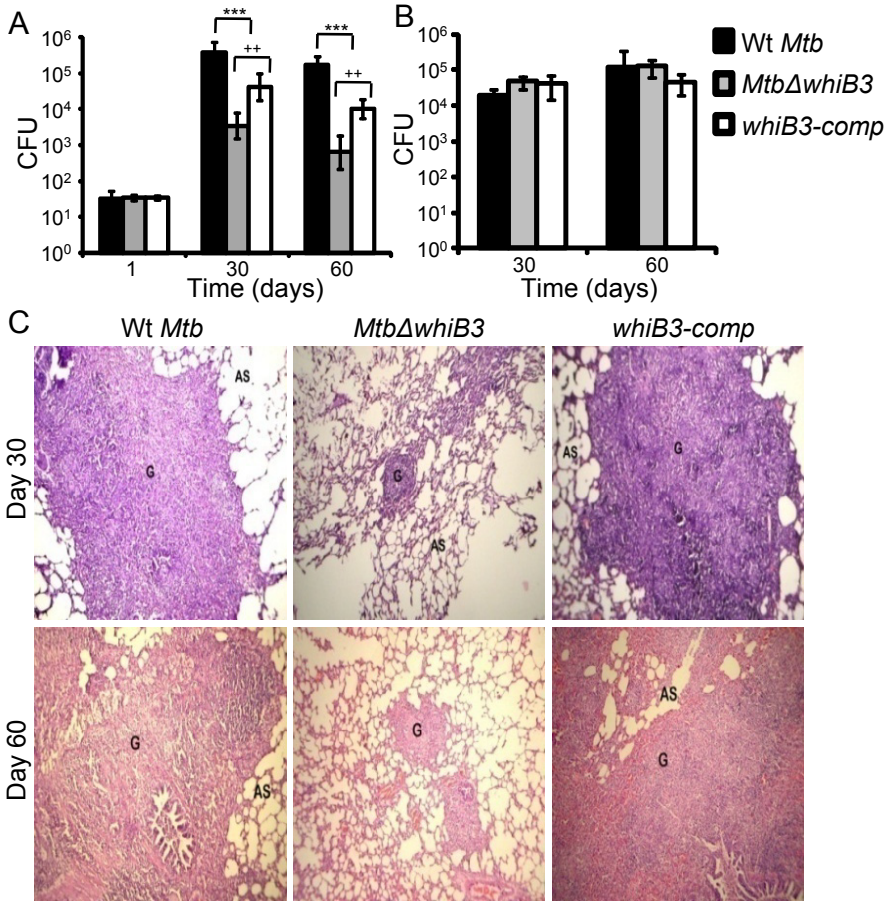

Fig. 9

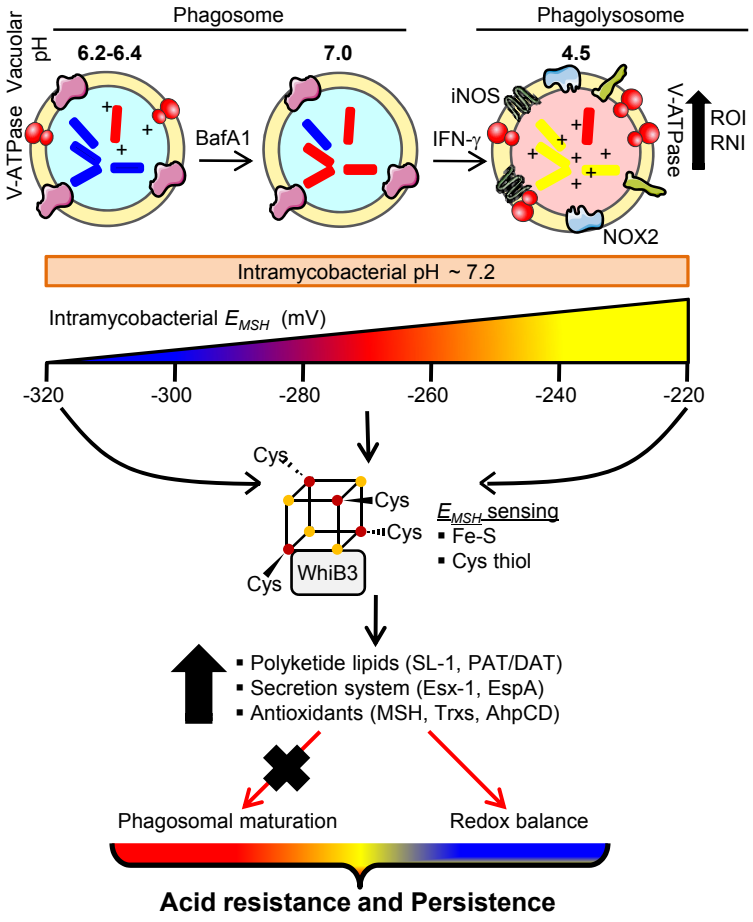

Fig. 10

Molecular Bases of Disease:

Mycobacterium tuberculosis WhiB3 responds to vacuolar pH- induced changes in mycothiol redox potential to modulate phagosomal maturation and virulence

Mansi Mehta, Raju S. Rajmani and Amit Singh

J. Biol. Chem. published online December 4, 2015